
How Transformers Utilize Multi-Head Attention in In-Context Learning? A Case Study on Sparse Linear Regression

Anonymous Authors¹

Abstract

In this study, we investigate how a trained multi-head transformer performs in-context learning on sparse linear regression. We experimentally discover distinct patterns in multi-head utilization across layers: multiple heads are essential in the first layer, while subsequent layers predominantly utilize a single head. We propose that the first layer preprocesses input data, while later layers execute simple optimization steps on the preprocessed data. Theoretically, we prove such a preprocess-then-optimize algorithm can outperform naive gradient descent and ridge regression, corroborated by experiments. Our findings provide insights into the benefits of multi-head attention and the intricate mechanisms within trained transformers.

1. Introduction

Transformers (Vaswani et al., 2023) have shown remarkable performance in natural language processing (Ouyang et al., 2022; Achiam et al., 2023; Brown et al., 2020; Radford et al., 2019) and other domains (Dosovitskiy et al., 2020; Peebles & Xie, 2023), exhibiting capabilities like in-context learning (Brown et al., 2020; Xie et al., 2021). While numerous studies have explored transformers’ expressive power (Kajitsuka & Sato, 2023; Takakura & Suzuki, 2023) and ability to emulate algorithms (Guo et al., 2023; Bai et al., 2023; Li et al.; Chen & Zou, 2024), understanding their inner workings remains a challenge, especially the roles of different attention layers and heads.

This work investigates how transformers utilize multi-head attention across layers for in-context learning on sparse linear regression tasks. Empirically, we observed a distinct

pattern: while the first attention layer utilized all heads evenly, subsequent layers predominantly relied on a single head. This suggests different working mechanisms for the first and later layers. Based on these findings, we propose that transformers employ a preprocess-then-optimize algorithm: the first layer preprocesses input data using multiple heads, then subsequent layers perform iterative optimization (e.g., gradient descent) on the preprocessed data using a single head. We theoretically demonstrate that such an algorithm can be implemented by a modestly-sized transformer and achieve lower excess risk than traditional methods like gradient descent and ridge regression without preprocessing.

Our main contributions are:

- We empirically revealing the distinct head utilization patterns across layers.
- Building upon our empirical findings, we proposed a possible working mechanism for multi-head transformers.
- We further validated our proposed mechanism by theoretical analysis.
- We conducted additional experiments to further validate our theoretical framework.

2. Preliminaries

Sparse Linear Regression. We consider sparse linear models where $(\mathbf{x}, y) \sim P = P_{\mathbf{w}^*}^{\text{lin}}$ is sampled as $\mathbf{x} \sim N(\mathbf{0}, \Sigma)$, $y = \langle \mathbf{w}^*, \mathbf{x} \rangle + N(0, \sigma^2)$, where the Σ is a diagonal matrix and ground truth $\mathbf{w}^* \in \mathbb{R}^d$ satisfies $\|\mathbf{w}^*\|_0 \leq s$. Then, we define the population risk of a parameter \mathbf{w} as:

$$L(\mathbf{w}) := \mathbb{E}_{(\mathbf{x}, y) \sim P} [(\langle \mathbf{x}, \mathbf{w} \rangle - y)^2].$$

Moreover, we are interested in the excess risk:

$$\mathcal{E}(\mathbf{w}) := L(\mathbf{w}) - \min_{\mathbf{w}} L(\mathbf{w}).$$

Linear Attention-only Transformers To perform an intractable theoretical investigation on the role of multi-head in the attention layer, we make simplifications on the transformer model by considering linear attention-only transformers. These simplifications are widely adopted in many

¹Anonymous Institution, Anonymous City, Anonymous Region, Anonymous Country. Correspondence to: Anonymous Author <anon.email@domain.com>.

Preliminary work. Under review by the International Conference on Machine Learning (ICML). Do not distribute.

recent works to study the behavior of transformer models (von Oswald et al., 2023; Zhang et al., 2023; Mahankali et al., 2023; Ahn et al.; Wu et al., 2023). In particular, the i -th layer TF_i performs the following update on the input sequence (or hidden state) $\mathbf{H}^{(i-1)}$ as follows:

$$\begin{aligned} \mathbf{H}^{(i)} &= \text{TF}_i(\mathbf{H}^{(i-1)}) \\ &= \mathbf{W}_1(\mathbf{H}^{(i-1)} + \text{Concat}[\{\mathbf{V}_i \mathbf{M} \mathbf{K}_i^\top \mathbf{Q}_i\}_{i=1}^h]), \\ \mathbf{M} &:= \begin{pmatrix} \mathbf{I}_n & \mathbf{0} \\ \mathbf{0} & \mathbf{0} \end{pmatrix} \in \mathbb{R}^{m \times m}, \end{aligned} \quad (2.1)$$

where $\{\mathbf{W}_{V_i}, \mathbf{W}_{K_i}, \mathbf{W}_{Q_i} \in \mathbb{R}^{\frac{d_{\text{hid}}}{h} \times d_{\text{hid}}}\}_{i=1}^h$ and $\mathbf{W}_1 \in \mathbb{R}^{d_{\text{hid}} \times d_{\text{hid}}}$ are learnable parameters. Besides, the mask matrix \mathbf{M} is included in the attention to constrain the model focus the first n in-context examples rather than the subsequent $m - n$ queries (Ahn et al.; Mahankali et al., 2023). To adapt the transformer for solving sparse linear regression problems, we introduce additional linear layers $\mathbf{W}_E \in \mathbb{R}^{(d+1) \times d_{\text{hid}}}$ and $\mathbf{W}_O \in \mathbb{R}^{d_{\text{hid}} \times 1}$ for input embedding and output projection, respectively. Mathematically, let \mathbf{E} denotes the input sequences with n in-context example followed by q queries,

$$\mathbf{E} = \begin{pmatrix} \mathbf{x}_1 & \mathbf{x}_2 & \cdots & \mathbf{x}_n & \mathbf{x}_{n+1} & \cdots & \mathbf{x}_{n+q} \\ y_1 & y_2 & \cdots & y_n & 0 & \cdots & 0 \end{pmatrix}. \quad (2.2)$$

Then model processes the input sequence \mathbf{E} , resulting in the output $\hat{\mathbf{y}} \in \mathbb{R}^{1 \times (n+q)}$:

$$\hat{\mathbf{y}} = \mathbf{W}_O \circ \text{TF}_L \circ \cdots \circ \text{TF}_1 \circ \mathbf{W}_E(\mathbf{E}),$$

here, L is the layer number of the transformer, and \hat{y}_{i+n} is the prediction value for the query \mathbf{x}_{i+n} . During training, we set $q > 1$ for efficiency, and for inference and theoretical analysis, we set $q = 1$ and define the in-context learning excess risk \mathcal{E}_{ICL} as:

$$\mathcal{E}_{\text{ICL}} := \mathbb{E}_{(\mathbf{x}, y) \sim P} (\hat{y}_{n+1} - y_{n+1})^2 - \sigma^2.$$

3. Experimental Insights into Multi-head Attention for In-context Learning

To understand the hidden mechanism behind the trained transformer, we design a series of experiments, utilizing techniques like probing (Alain & Bengio, 2016) and pruning (Li et al., 2017) to help us gain initial insights into how the trained transformer utilizes multi-head attention.

ICL with Varying Heads: This experiment investigates the performance of transformers in solving in-context sparse linear regression with different numbers of attention heads. An example can be found in Figure 1b, where we display the excess risk for different models when using different

numbers of in-context examples. We can observe that given few-shot in-context examples, transformers can outperform OLS and ridge. Moreover, we can also clearly observe the benefit of using multiple heads, which leads to lower excess risk when increasing the number of heads. This **highlights the importance of multi-head attention in transformer to perform in-context learning.**

Heads Assessment: This experiment evaluates the importance of each attention head by masking individual heads and measuring the change in risk. An example can be found in Figure 1c. We find that in the first layer, no head distinctly outweighs the others, while in the subsequent layers, there always exists a head that exhibits higher importance than others. This gives us insight that **in the first attention layer, all heads appear to be significant, while in the subsequent layers, only one head appears to be significant.**

Pruning and Probing: Based on the previous findings, this experiment prunes the trained model by retaining all heads in the first layer and only keeping the most important head in subsequent layers. The pruned model is then fine-tuned. Linear probes are used to evaluate the prediction performance of different layers. An example can be found in Figure 1d, it shows that the pruned model performs similarly to the original model, but differently from a single-head transformer. Noting that the main difference between them is the number of heads in the first layer (subsequent layers have the same structure), it can be deduced that **the working mechanisms of the multi-head transformer may be different for the first and subsequent layers.**

4. Potential Mechanism Behind Trained transformer

Based on the experimental insights from Section 3, we found that while all heads in the first layer are crucial, only one head plays a significant role in subsequent layers. Additionally, probing and pruning results suggest different working mechanisms for the first and subsequent layers. To this end, we hypothesize that the multi-layer transformer implements a preprocess-then-optimize approach for in-context learning, where the first layer preprocesses the in-context examples, and subsequent layers implement iterative optimization algorithms on the preprocessed data.

4.1. Preprocessing on In-context Examples

As the multihead attention is designed to facilitate to model to capture features from different representation subspaces (Vaswani et al., 2023), we abstract the algorithm implementation by the first layer of the transformers as a preprocessing procedure. In general, for the sparse linear regression, a

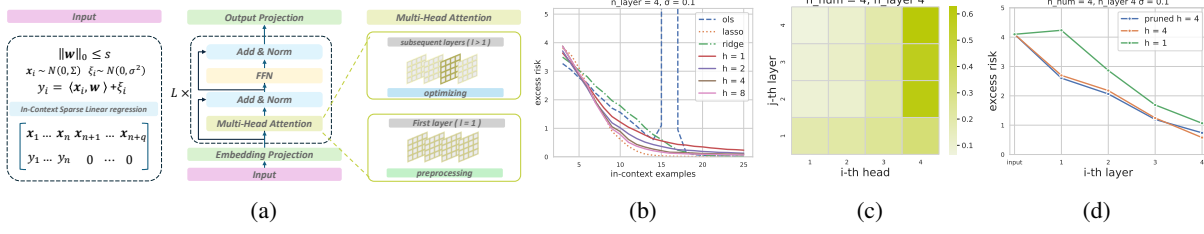


Figure 1: Experimental insights into multi-head attention for in-context learning. (a): Overview of the experiments, including task, data, architecture, and our insights. (b): ICL with Varying Heads. (c): Heads Assessment. (d): Pruning and Probing.

possible data preprocessing method is to perform reweighting of the data features by emphasizing the features that correspond to the nonzero entries of the ground truth w^* and disregard the remaining features. In the idealized case, if we know the nonzero support of w^* , we can trivially zero out the data features of x on the complement of the nonzero support, as a data preprocessing procedure, and perform projected gradient descent to obtain the optimal solution. Although the nonzero support of w^* is intractable to the learner, we can estimate each dimension w_i^* by $\frac{1}{n} \sum_{i=1}^n x_{ij} y_i$, as $\mathbb{E}[x_i y] = \mathbb{E}[\sum_{i=1}^d w_i^* x_i \cdot x_i] + \mathbb{E}[\xi x_i] = w_i^* \mathbb{E}[x_i^2]$, resulting in Alg. 1.

4.2. Optimizing Over Preprocessed In-Context Examples

Based on the experimental results, we observe that the subsequent layers of transformers dominantly rely on one single head, suggesting their different but potentially simpler behavior compared to the first one. Motivated by a series of recent work (von Oswald et al., 2023; Cheng et al., 2023; Zhang et al., 2023) that reveal the connection between gradient descent steps and multi-layer single-head transformer in the in-context learning tasks, we conjecture that the subsequent layers also implement iterative optimization algorithms, e.g., gradient descent algorithm, on the (preprocessed) in-context examples.

We further prove that these two procedures (preprocessing then optimizing) can be implemented by linear attention-only transformers in Propositions C.1 and C.2 (presented in Appendix). More details about our preprocess-then-optimize algorithm can be found in Appendix C.

5. Excess Risk of the Preprocess-then-optimize Algorithm

In this section, we will develop the theory to demonstrate the improved performance of the preprocess-then-optimize algorithm compared to the gradient descent algorithm on the raw inputs. Appendix E provides a more detailed analysis.

We first denote \tilde{w}_{gd}^t as the estimator obtained by t -step

Algorithm 1 Data preprocessing for in-context examples

- 1: **Input** : Sequence with $\{(x_i, y_i)\}_{i=1}^n, \{(x_i, 0)\}_{i=n+1}^{n+q}$ as in-context examples/queries.
- 2: **for** $k = 1, \dots, n$ **do**
- 3: Compute \tilde{x}_k by $\tilde{x}_k = \hat{\mathbf{R}} x_k$,
 where $\hat{\mathbf{R}} = \text{diag}\{\hat{r}_1, \hat{r}_2, \dots, \hat{r}_d\}$, where \hat{r}_j is given by

$$\hat{r}_j = \frac{1}{n} \sum_{i=1}^n x_{ij} y_i. \quad (4.1)$$
- 4: **end for**
- 5: **Output** : Sequence with the preprocessed in-context examples/queries $\{(\tilde{x}_i, y_i)\}_{i=1}^n, \{(\tilde{x}_i, 0)\}_{i=n+1}^{n+q}$.

GD on $\{(\tilde{x}_i, y_i)\}_{i=1}^n$, which can be viewed as the solution generated by the $t + 1$ -layer transformer based on our discussion in Section 4, and w_{gd}^t as the estimator obtained by t -step GD on $\{(x_i, y_i)\}_{i=1}^n$. Before presenting our main theorem, we first need to redefine the excess risk of GD on $\{(\tilde{x}_i, y_i)\}_{i=1}^n$. Note that in our algorithm, the learned predictor takes the form $x \rightarrow \langle \hat{\mathbf{R}} x, \tilde{w}_{\text{gd}}^t \rangle$. Consequently, the population risk of a parameter \tilde{w}_{gd}^t is naturally defined as $\tilde{L}(\tilde{w}_{\text{gd}}^t) := \frac{1}{2} \cdot \mathbb{E}_{(x, y) \sim \mathcal{P}} [(\langle \hat{\mathbf{R}} x, \tilde{w}_{\text{gd}}^t \rangle - y)^2]$, and the excess risk is then defined as $\mathcal{E}(w) := \tilde{L}(w) - \min_w \tilde{L}(w)$ ¹.

To make a formal comparison between preprocess-then-optimize and baselines, we consider the example where $x_i \stackrel{\text{i.i.d.}}{\sim} N(\mathbf{0}, \mathbf{I})$, based on which we can get the upper bound for our algorithm and the lower bound for OLS, ridge regression, and finite-step GD.

Theorem 5.1. *Suppose \mathcal{S} with $|\mathcal{S}| = s$ is selected such that each element is chosen with equal probability from the set $\{1, 2, \dots, d\}$ and $w_i^* \sim U\{-1/\sqrt{s}, 1/\sqrt{s}\}$ has a restricted uniform prior for $i \in \mathcal{S}$, $\|w^*\|_2 \simeq \Theta(1)$ and $n \gtrsim t^2 s^3 d^{2/3}$.*

¹Here for the ease of presentation and comparison, we slightly abuse the notation of $\mathcal{E}(w)$ by extending it to \tilde{w}_{gd}^t , although $\mathcal{E}(w)$ is originally defined for the estimator for the raw feature vector x .

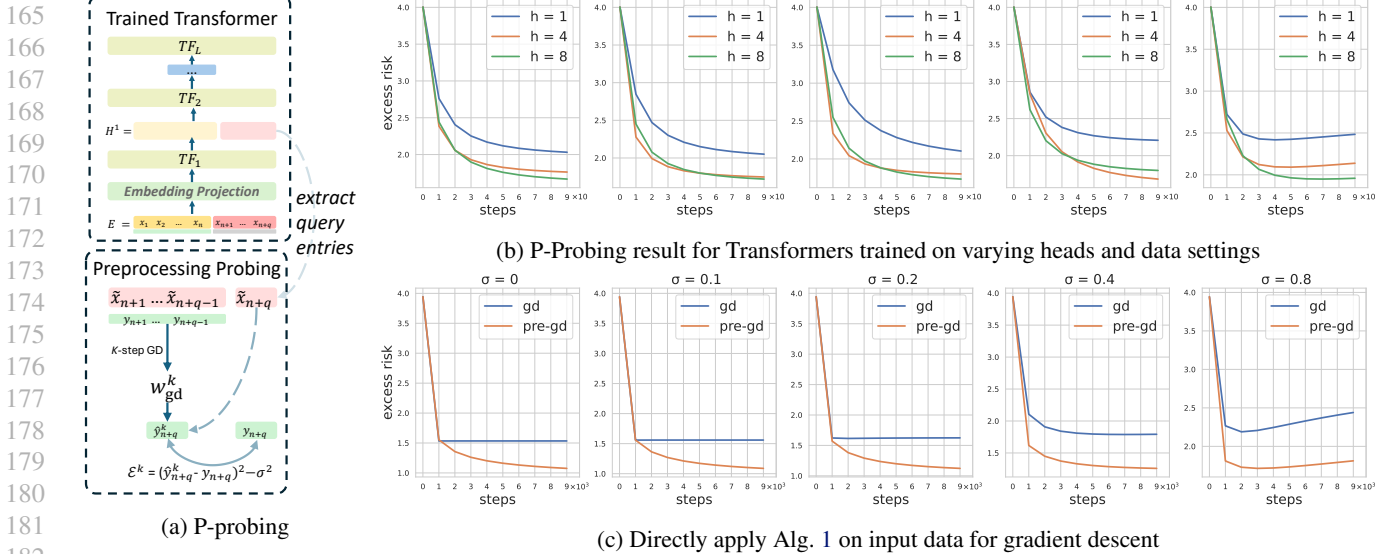


Figure 2: Supporting experiments for our preprocess-then-optimize algorithm and theoretical analysis

Then there exists a choice of η and t such that

$$\mathcal{E}(\tilde{\mathbf{w}}_{\text{gd}}^t) \lesssim \sigma^2 \log^2(ns/\sigma^2) \log^2(d/\delta) \cdot \left(\frac{s}{n} + \frac{ds^2}{n^2} \right),$$

with probability at least $1 - \delta$. Besides, let $\hat{\mathbf{w}}_\lambda$ be the ridge regression estimator with regularized parameter λ , and \mathbf{w}_{ols} be the OLS estimator, it holds that

$$\mathbb{E}_{\mathbf{w}^*}[\mathcal{E}(\mathbf{w})] \gtrsim \begin{cases} \frac{\sigma^2 d}{n} & n \gtrsim d + \log(1/\delta) \\ 1 - \frac{n}{d} + \frac{\sigma^2 n}{d} & d \gtrsim n + \log(1/\delta), \end{cases}$$

with probability at least $1 - \delta$, where $\mathbf{w} \in \{\hat{\mathbf{w}}_\lambda, \mathbf{w}_{\text{ols}}, \mathbf{w}_{\text{gd}}^t\}$.

It can be seen that for a wide range of under-parameterized and over-parameterized cases, $\tilde{\mathbf{w}}_{\text{gd}}^t$ has a smaller excess risk than ridge regression, standard gradient descent, and OLS, when the sparsity s satisfies $s = o(\min\{d, n\})$. This justifies the effectiveness of the preprocess-then-optimize algorithm for dealing with the sparse regression problem. Moreover, it is well known that Lasso can achieve $\tilde{O}(s/n)$ excess risk bound in the setting of Theorem 5.1. Then we can conclude that the preprocess-then-optimize algorithm can be comparable to Lasso up to logarithmic factors when $d \lesssim n$, while becomes worse when $d \gtrsim n$.

6. Experiments

In Section 3, we conduct several experiments, and based on the observations, we propose that a trained transformer can apply a preprocess-then-optimize algorithm. While the second part (gradient descent over context) is supported by extensive theoretical analysis and experimental evidence (von Oswald et al., 2023; Cheng et al., 2023; Zhang et al.,

2023; Ahn et al.), here we develop a technique called preprocess-then-optimize (P-probing) on the trained transformer to support the first part of our algorithm, where we try to extract the preprocessed component $\{\tilde{\mathbf{x}}_i\}_{i=n+1}^{n+q}$ from the first layer of transformer as in, as illustrated in Figure 2a. We also directly apply Alg. 1 on the in-context examples and then check the excess risk for multiple-step gradient descent to verify the effectiveness of our algorithm and theoretical analysis. Experimental details can be found in Appendix A.

Based on Figure 2b, we can observe that compared to the transformer with single-head attention ($h = 1$), the query entries extracted from the transformer with multiple heads ($h = 4, 8$) preserve better convergence performance and can dive into a lower risk. This aligns well with our experiment result in Figure 2c, where compared to gd , the data preprocessed by Alg. 1 preserves better convergence performance and can dive into a lower risk space, supporting the existence of the preprocessing procedure in the trained transformer. Moreover, Figure 2c also aligns well with our theoretical analysis, where our algorithm can outperform ridge regression and OLS.

7. Conclusions

In this paper, we investigate a sparse linear regression problem and explore how a trained transformer leverages multi-head attention for in-context learning. Based on the experiment and theoretical characterizations, we show that transformer may implement the preprocess-then-optimize algorithm, by using multiple heads in the first layer and one head in the subsequent layer. Numerical experiments support our findings.

References

- 220
221
222 Achiam, J., Adler, S., Agarwal, S., Ahmad, L., Akkaya, I.,
223 Aleman, F. L., Almeida, D., Altenschmidt, J., Altman, S.,
224 Anadkat, S., et al. Gpt-4 technical report. *arXiv preprint*
225 *arXiv:2303.08774*, 2023.
- 226
227 Ahn, K., Cheng, X., Daneshmand, H., and Sra, S. Trans-
228 formers learn to implement preconditioned gradient de-
229 scent for in-context learning.
- 230
231 Alain, G. and Bengio, Y. Understanding intermediate
232 layers using linear classifier probes. *arXiv preprint*
233 *arXiv:1610.01644*, 2016.
- 234
235 Allen-Zhu, Z. and Li, Y. Physics of language mod-
236 els: Part 3.2, knowledge manipulation. *arXiv preprint*
237 *arXiv:2309.14402*, 2023.
- 238
239 Bai, Y., Chen, F., Wang, H., Xiong, C., and Mei, S. Trans-
240 formers as Statisticians: Provable In-Context Learning
241 with In-Context Algorithm Selection, July 2023.
- 242
243 Bartlett, P. L., Long, P. M., Lugosi, G., and Tsigler, A.
244 Benign overfitting in linear regression. *Proceedings of*
245 *the National Academy of Sciences*, 117(48):30063–30070,
246 2020.
- 247
248 Bills, S., Cammarata, N., Mossing, D., Tillman, H., Gao, L.,
249 Goh, G., Sutskever, I., Leike, J., Wu, J., and Saunders,
250 W. Language models can explain neurons in language
251 models. URL <https://openaipublic.blob.core.windows.net/neuron-explainer/paper/index.html>. (Date accessed:
252 14.05. 2023), 2023.
- 253
254
255 Bricken, T., Templeton, A., Batson, J., Chen, B., Jermyn, A.,
256 Conerly, T., Turner, N., Anil, C., Denison, C., Askell, A.,
257 et al. Towards monosemanticity: Decomposing language
258 models with dictionary learning. *Transformer Circuits*
259 *Thread*, pp. 2, 2023.
- 260
261 Brown, T., Mann, B., Ryder, N., Subbiah, M., Kaplan, J. D.,
262 Dhariwal, P., Neelakantan, A., Shyam, P., Sastry, G.,
263 Askell, A., et al. Language models are few-shot learners.
264 *Advances in neural information processing systems*, 33:
265 1877–1901, 2020.
- 266
267 Chen, X. and Zou, D. What can transformer learn with
268 varying depth? case studies on sequence learning tasks.
269 *arXiv preprint arXiv:2404.01601*, 2024.
- 270
271 Cheng, X., Chen, Y., and Sra, S. Transformers implement
272 functional gradient descent to learn non-linear functions
273 in context. *arXiv preprint arXiv:2312.06528*, 2023.
- 274
275
276
277
278
279
280
281
282
283
284
285
286
287
288
289
290
291
292
293
294
295
296
297
298
299
300
301
302
303
304
305
306
307
308
309
310
311
312
313
314
315
316
317
318
319
320
321
322
323
324
325
326
327
328
329
330
331
332
333
334
335
336
337
338
339
340
341
342
343
344
345
346
347
348
349
350
351
352
353
354
355
356
357
358
359
360
361
362
363
364
365
366
367
368
369
370
371
372
373
374
375
376
377
378
379
380
381
382
383
384
385
386
387
388
389
390
391
392
393
394
395
396
397
398
399
400
401
402
403
404
405
406
407
408
409
410
411
412
413
414
415
416
417
418
419
420
421
422
423
424
425
426
427
428
429
430
431
432
433
434
435
436
437
438
439
440
441
442
443
444
445
446
447
448
449
450
451
452
453
454
455
456
457
458
459
460
461
462
463
464
465
466
467
468
469
470
471
472
473
474
475
476
477
478
479
480
481
482
483
484
485
486
487
488
489
490
491
492
493
494
495
496
497
498
499
500
501
502
503
504
505
506
507
508
509
510
511
512
513
514
515
516
517
518
519
520
521
522
523
524
525
526
527
528
529
530
531
532
533
534
535
536
537
538
539
540
541
542
543
544
545
546
547
548
549
550
551
552
553
554
555
556
557
558
559
560
561
562
563
564
565
566
567
568
569
570
571
572
573
574
575
576
577
578
579
580
581
582
583
584
585
586
587
588
589
590
591
592
593
594
595
596
597
598
599
600
601
602
603
604
605
606
607
608
609
610
611
612
613
614
615
616
617
618
619
620
621
622
623
624
625
626
627
628
629
630
631
632
633
634
635
636
637
638
639
640
641
642
643
644
645
646
647
648
649
650
651
652
653
654
655
656
657
658
659
660
661
662
663
664
665
666
667
668
669
670
671
672
673
674
675
676
677
678
679
680
681
682
683
684
685
686
687
688
689
690
691
692
693
694
695
696
697
698
699
700
701
702
703
704
705
706
707
708
709
710
711
712
713
714
715
716
717
718
719
720
721
722
723
724
725
726
727
728
729
730
731
732
733
734
735
736
737
738
739
740
741
742
743
744
745
746
747
748
749
750
751
752
753
754
755
756
757
758
759
760
761
762
763
764
765
766
767
768
769
770
771
772
773
774
775
776
777
778
779
780
781
782
783
784
785
786
787
788
789
790
791
792
793
794
795
796
797
798
799
800
801
802
803
804
805
806
807
808
809
810
811
812
813
814
815
816
817
818
819
820
821
822
823
824
825
826
827
828
829
830
831
832
833
834
835
836
837
838
839
840
841
842
843
844
845
846
847
848
849
850
851
852
853
854
855
856
857
858
859
860
861
862
863
864
865
866
867
868
869
870
871
872
873
874
875
876
877
878
879
880
881
882
883
884
885
886
887
888
889
890
891
892
893
894
895
896
897
898
899
900
901
902
903
904
905
906
907
908
909
910
911
912
913
914
915
916
917
918
919
920
921
922
923
924
925
926
927
928
929
930
931
932
933
934
935
936
937
938
939
940
941
942
943
944
945
946
947
948
949
950
951
952
953
954
955
956
957
958
959
960
961
962
963
964
965
966
967
968
969
970
971
972
973
974
975
976
977
978
979
980
981
982
983
984
985
986
987
988
989
990
991
992
993
994
995
996
997
998
999
1000

- 275 with human feedback. *Advances in neural information*
 276 *processing systems*, 35:27730–27744, 2022.
- 277 Pandit, O. and Hou, Y. Probing for bridging infer-
 278 ence in transformer language models. *arXiv preprint*
 279 *arXiv:2104.09400*, 2021.
- 280 Peebles, W. and Xie, S. Scalable diffusion models with
 281 transformers. In *Proceedings of the IEEE/CVF Interna-*
 282 *tional Conference on Computer Vision*, pp. 4195–4205,
 283 2023.
- 284 Radford, A., Wu, J., Child, R., Luan, D., Amodei, D.,
 285 Sutskever, I., et al. Language models are unsupervised
 286 multitask learners. *OpenAI blog*, 1(8):9, 2019.
- 287 Takakura, S. and Suzuki, T. Approximation and Estima-
 288 tion Ability of Transformers for Sequence-to-Sequence
 289 Functions with Infinite Dimensional Input, May 2023.
- 290 Tarzanagh, D. A., Li, Y., Thrampoulidis, C., and Oymak,
 291 S. Transformers as Support Vector Machines, September
 292 2023.
- 293 Tian, Y., Wang, Y., Chen, B., and Du, S. Scan and Snap: Un-
 294 derstanding Training Dynamics and Token Composition
 295 in 1-layer Transformer, July 2023.
- 296 Tsigler, A. and Bartlett, P. L. Benign overfitting in ridge
 297 regression. *Journal of Machine Learning Research*, 24
 298 (123):1–76, 2023.
- 299 Vaswani, A., Shazeer, N., Parmar, N., Uszkoreit, J., Jones,
 300 L., Gomez, A. N., Kaiser, L., and Polosukhin, I. Attention
 301 Is All You Need, August 2023.
- 302 Vershynin, R. High-dimensional probability. *University of*
 303 *California, Irvine*, 10:11, 2020.
- 304 von Oswald, J., Niklasson, E., Randazzo, E., Sacramento,
 305 J., Mordvintsev, A., Zhmoginov, A., and Vladymyrov, M.
 306 Transformers learn in-context by gradient descent, May
 307 2023.
- 308 Weiss, G., Goldberg, Y., and Yahav, E. Thinking Like
 309 Transformers, July 2021.
- 310 Wolf, T., Debut, L., Sanh, V., Chaumond, J., Delangue, C.,
 311 Moi, A., Cistac, P., Rault, T., Louf, R., Funtowicz, M.,
 312 et al. Huggingface’s transformers: State-of-the-art natural
 313 language processing. *arXiv preprint arXiv:1910.03771*,
 314 2019.
- 315 Wu, J., Zou, D., Chen, Z., Braverman, V., Gu, Q., and
 316 Bartlett, P. How many pretraining tasks are needed for
 317 in-context learning of linear regression? In *The Twelfth*
 318 *International Conference on Learning Representations*,
 319 2023.
- 320 Wu, Z., Chen, Y., Kao, B., and Liu, Q. Perturbed masking:
 321 Parameter-free probing for analyzing and interpreting
 322 bert. *arXiv preprint arXiv:2004.14786*, 2020.
- 323 Xie, S. M., Raghunathan, A., Liang, P., and Ma, T. An
 324 explanation of in-context learning as implicit bayesian
 325 inference. In *International Conference on Learning Rep-*
 326 *resentations*, 2021.
- 327 Zhang, R., Frei, S., and Bartlett, P. L. Trained trans-
 328 formers learn linear models in-context. *arXiv preprint*
 329 *arXiv:2306.09927*, 2023.
- Zhou, H., Bradley, A., Littwin, E., Razin, N., Saremi, O.,
 Susskind, J. M., Bengio, S., and Nakkiran, P. What
 algorithms can transformers learn? a study in length
 generalization. In *The Twelfth International Conference*
on Learning Representations, 2024. URL [https://](https://openreview.net/forum?id=AssIuHnmHX)
openreview.net/forum?id=AssIuHnmHX.
- Zhu, Z. A. and Li, Y. Physics of language models: Part
 3.1, knowledge storage and extraction. *arXiv preprint*
arXiv:2309.14316, 2023.
- Zou, D., Wu, J., Braverman, V., Gu, Q., Foster, D. P., and
 Kakade, S. The benefits of implicit regularization from
 sgd in least squares problems. *Advances in neural infor-*
mation processing systems, 34:5456–5468, 2021.
- Zou, D., Wu, J., Braverman, V., Gu, Q., and Kakade, S.
 Risk bounds of multi-pass sgd for least squares in the
 interpolation regime. *Advances in Neural Information*
Processing Systems, 35:12909–12920, 2022.

A. Additional Details for Sections 3 and 6

Architecture and Optimization We conduct extensive experiments on encoder-only transformers with $d_{\text{hid}} = 256$, varying the number of heads $h \in \{1, 2, 4, 8\}$, layers $l \in \{3, 4, 5, 6\}$, and noise levels $\sigma \in \{0, 0.1, 0.2, 0.4, 0.8\}$. For the input sequence, we sample $\mathbf{x} \sim \mathcal{N}(\mathbf{0}, \mathbf{I})$. For \mathbf{w} , we first sample $\mathbf{w} \sim \mathcal{N}(\mathbf{0}, \mathbf{I}) \in \mathbb{R}^{16}$, and randomly choose $s = 4$ entries, setting the other elements to zero. Note that We don't apply positional encodings in our setting, as no positional information is needed in our input setting. To further support our preprocessing-then-optimize algorithm, we also try a decoder-only architecture(Figure 9) and train models with $s = d = 16$ (Figure 10) as a comparison in Appendix I. During training, we set $n = 12$ and $q = 4$, with a batch size of 64. We utilize the Adam optimizer with a learning rate $\gamma = 10^{-4}$ for 320000 updates. Each experiment takes about two hours on a single NVIDIA GeForce RTX 4090 GPU. We fix the random seed such that each model is trained and evaluated with the same training and evaluation dataset. We use HuggingFace (Wolf et al., 2019) library to implement our models.

ICL with Varying Heads We compare the model's performance with ridge regression, OLS, and lasso. For ridge regression and lasso, we tune $\lambda, \alpha \in \{1, 10^{-1}, 10^{-2}, 10^{-3}, 10^{-4}\}$ respectively for the lowest risk, as in (Garg et al., 2023).

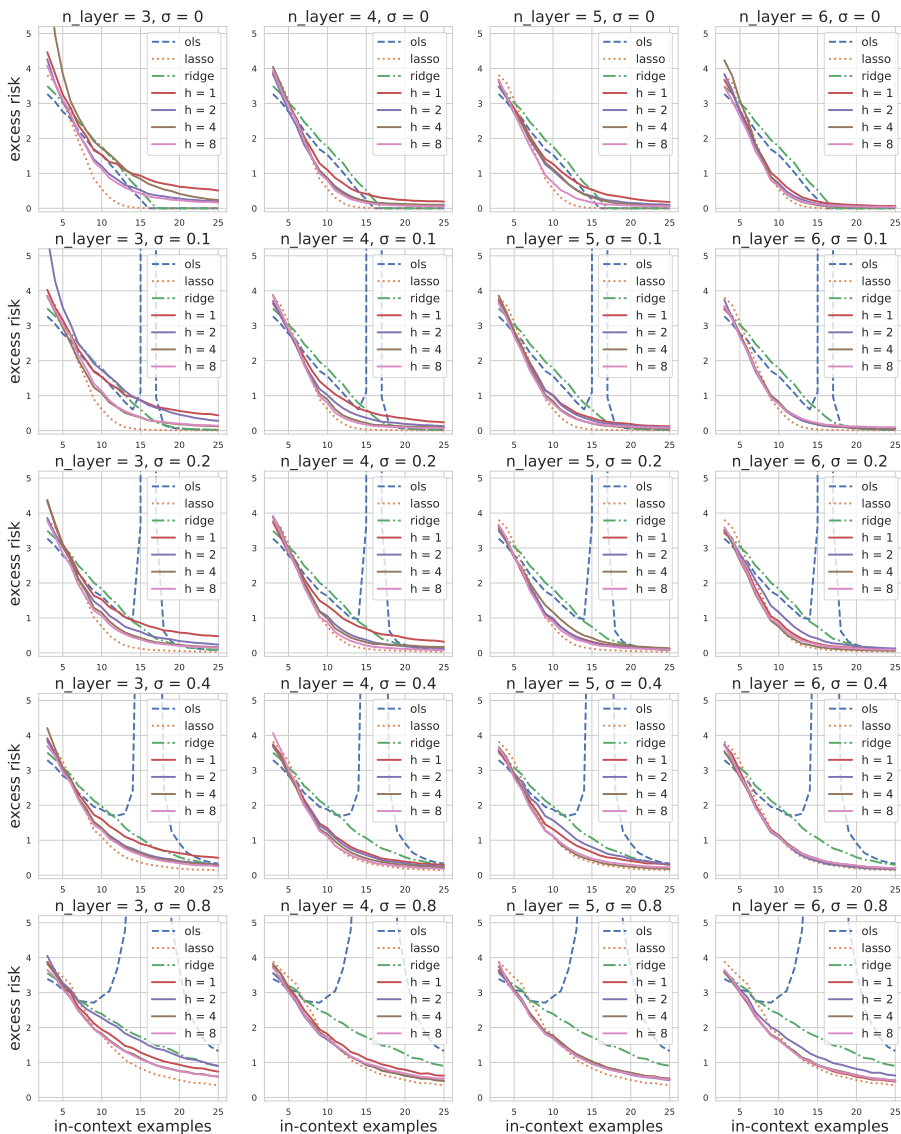


Figure 3: ICL with varying heads, layers and noise levels

From Figure 3, we can find that in most cases, transformers with single head ($h = 1$) exhibits higher risk compared to models with multiple heads ($h = 4, 8$). Note that in the same subplot, models with different numbers of heads have the same number of parameters. This experiment highlights the importance of multi-head attention for transformers in in-context learning.

Heads Assessment Based on Eq.(2.1), we know that the j -th head at the i -th layer corresponds to the subspace of the intermediate output from $(j - 1) \cdot d_{\text{hid}}/h$ to $j \cdot d_{\text{hid}}/h - 1$. To assess the importance of each attention head, we can mask the particular head by zeroing out the corresponding output entries, while keeping other dimensions unchanged. Then, let (i, j) be the layer and head indices, we evaluate the risk change before and after head masking, denoted by $\Delta\mathcal{E}_{\text{ICL}}(i, j)$. Then we normalize the risk changes in the same layer to evaluate their relative importance:

$$\mathcal{W}_{i,j} = \frac{\Delta\mathcal{E}_{\text{ICL}}(i,j)}{\sum_{k=1}^h \Delta\mathcal{E}_{\text{ICL}}(i,k)}. \tag{A.1}$$

Here, we set $n = 10$ and $q = 1$, with an evaluation data size of 8192. For a model with h heads and l layers, we train $|\sigma|$ models under different noise levels. We first compute the $\mathcal{W}^{h,l,\sigma}$ under different noise levels σ , then sort each row in $\mathcal{W}^{h,l,\sigma}$, and add them together as $\mathcal{W}_{\text{avg}}^{h,l} = \frac{1}{|\sigma|} \sum_{\sigma \in \sigma} \mathcal{W}^{h,l,\sigma}$, resulting in the final weight for each head. An example can be found in Fig 1c. In Fig 4, we present more results for different h and l , and we also present the heat map for the decode-only transformers in Figure 9.

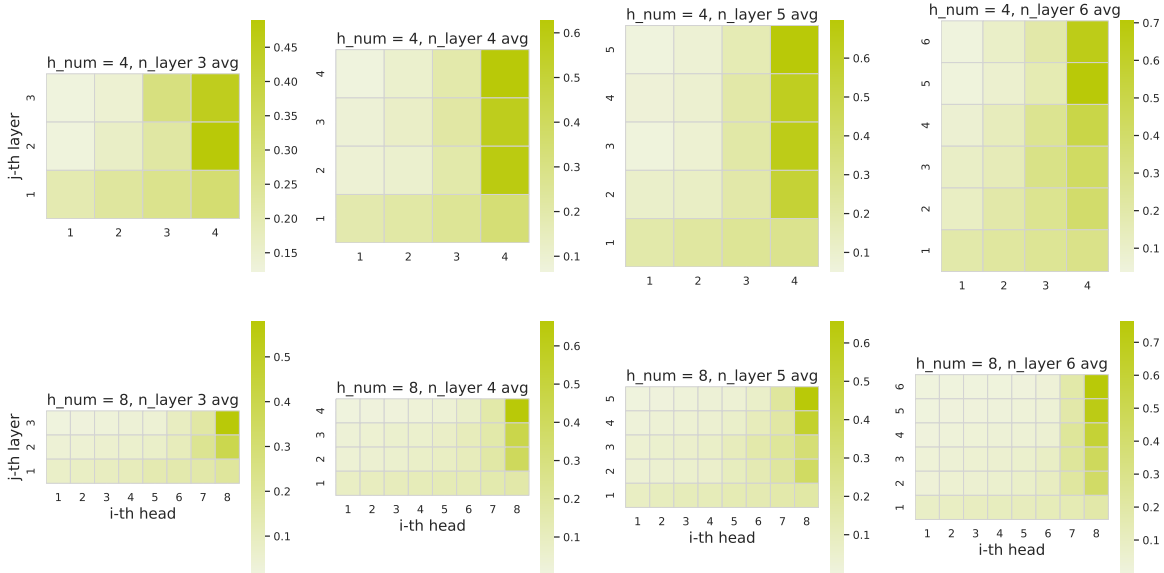


Figure 4: Head Assessment with varying heads, layers

From Fig 4, we can find that in most settings, each head contributes almost equally, while in the subsequent layers, there always exists a head that has a much larger weight than the others. This indicates that in trained transformers for in-context learning, in the first attention layer, all heads appear to be significant, while in the subsequent layers, only one head appears to be significant.

Pruning and Probing Here, we also set $n = 10$ and $q = 1$, with an evaluation data size of 8192. To further support our finding from the Head Assessment, we first prune the model based on our computed head weight $\mathcal{W}_{\text{avg}}^{h,l}$, where we keep all heads in the first layer, whereas we only keep the head with the highest score weight and mask the others. We then train the pruned model with the same method as before for 60000 steps. In Fig 5, 6, 7, 8, we provide the Pruning and Probing results for different numbers of heads $h \in \{4, 8\}$ and noise levels $\sigma \in \{0, 0.1, 0.2, 0.4, 0.8\}$. It can be found that in almost all cases, the pruned model exhibits almost the same performance in each layer, while being largely different from the single-layer

transformer. This further supports the results in the Heads Assessment and indicates that the working mechanisms of the multi-head transformer may be different for the first and subsequent layers.

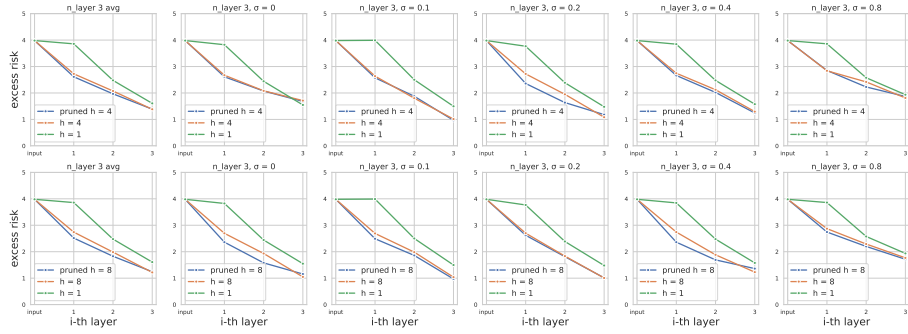


Figure 5: Pruning and Probing, 3 layers

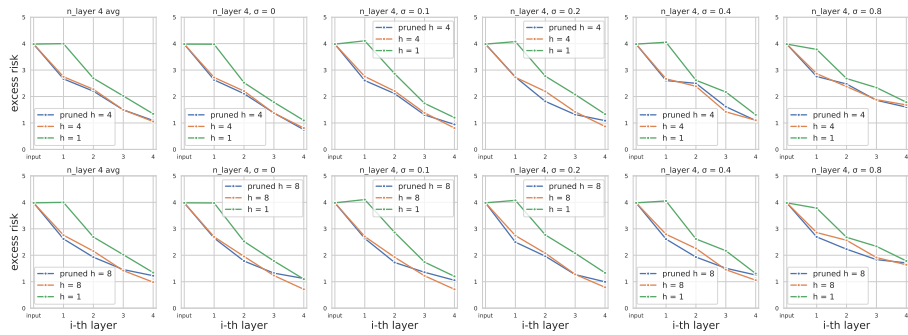


Figure 6: Pruning and Probing, 4 layers

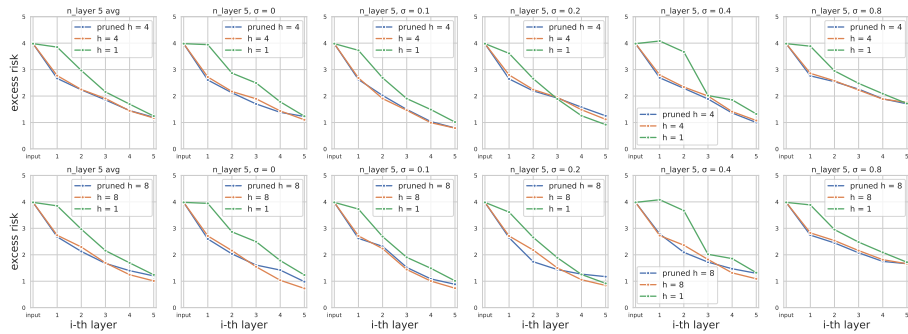


Figure 7: Pruning and Probing, 5 layers

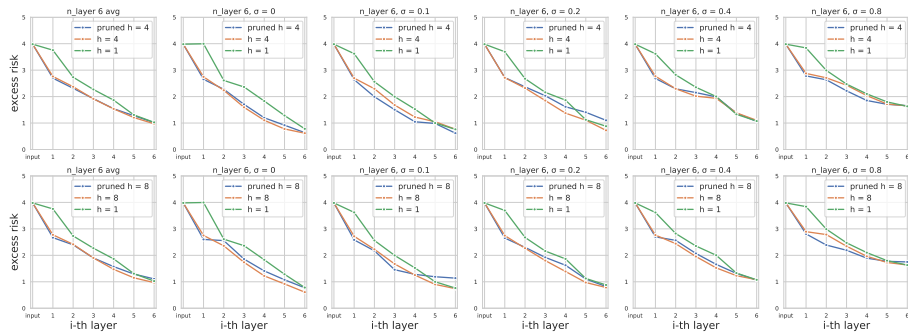


Figure 8: Pruning and Probing, 6 layers

P-probing: To verify the existence of a preprocessing procedure in the trained transformer, we develop a ‘‘preprocessing probing’’ (P-probing) technique on the trained transformers, as illustrated in Figure 2a. For a trained transformer, we first set the input sequence as in Eq.(2.2), where the first n examples $\{\mathbf{x}\}_{i=1}^n$ have the corresponding labels $\{y\}_{i=1}^n$, and the following q query entries only have $\{\mathbf{x}_i\}_{i=n+1}^{n+q}$ in the sequence. Then, we extract the last q vectors in the output hidden state \mathbf{H}^1 from the first layer of the transformer and treat these data as processed query entries. Next, we conduct gradient descent on the first $q - 1$ query entries with their corresponding y , computing the excess risk on the last query. Additional experimental details can be found in Appendix A. We adapt this technique based on the intuition that, according to our theoretical analysis, we can extract the preprocessed entry $\{\tilde{\mathbf{x}}_i\}_{i=n+1}^{n+q}$ from \mathbf{H}^1 , besides, the excess risk computed by the preprocessed data has a better upper bound guarantee compared to raw data without preprocessing under the same number of gradient descent steps, so if the trained transformer utilize multihead attention for preprocess, compared with single head attention, the queries entries extract from \mathbf{H}^1 by multihead attention can have better gradient descent performance compared with single head attention. Here, we also set $n = 117$ and $q = 11$, with an evaluation data size of 1024. We choose $n \gg q$ such that the model can handle more queries ($q = 11$) than those in the training ($q = 4$) process.

Verifying the benefit of preprocessing: To further support the effectiveness of our algorithm, we directly apply Alg. 1 on the input data $\{\mathbf{x}_i, y_i\}_{i=1}^{n+1}$, and then implement gradient descent on the example entries $\{\mathbf{x}_i, y_i\}_{i=1}^n$ and compute the excess risk with the last query $\{\tilde{\mathbf{x}}_{n+1}, y_{n+1}\}$, we refer this procedure as pre-gd. We compare pre-gd with the excess risk obtained by directly applying gradient descent without preprocessing (referred to as gd). For all experiments (both P-probing and this), we set $\mathbf{w}_{\text{gd}}^0 = \mathbf{0}$ and tune the learning rate η for each model by choosing from $[1, 10^{-1}, 10^{-2}, 10^{-3}, 10^{-4}, 10^{-5}, 10^{-6}]$ with the lowest average excess risk.

B. Theoretical Analysis of the Preprocess-then-optimize Algorithm

B.1. Notations

For two functions $f(x) \geq 0$ and $g(x) \geq 0$ defined on the positive real numbers ($x > 0$), we write $f(x) \lesssim g(x)$ if there exists two constants $c, x_0 > 0$ such that $\forall x \geq x_0, f(x) \leq c \cdot g(x)$; we write $f(x) \gtrsim g(x)$ if $g(x) \lesssim f(x)$; we write $f(x) \asymp g(x)$ if $f(x) \lesssim g(x)$ and $g(x) \lesssim f(x)$. If $f(x) \lesssim g(x)$, we can write $f(x)$ as $O(g(x))$. We can also write $f(x)$ as $\tilde{O}(g(x))$ if there exists a constant $k > 0$ such that $f(x) \lesssim g(x) \log^k(x)$.

B.2. Theoretical results

We first provide the upper bound of the excess risk for $\mathcal{E}(\tilde{\mathbf{w}}_{\text{gd}}^t)$ and $\mathcal{E}(\mathbf{w}_{\text{gd}}^t)$ respectively.

Theorem B.1. Denote $\mathcal{S} := \{i : w_i^* \neq 0\}$ and $\mathbf{R} = \text{diag}\{r_1, \dots, r_d\}$, where $r_j = \sum_{i=1}^d w_i^* \Sigma_{ij}$. Suppose that there exist a $\beta > 0$ such that $\min_{i \in \mathcal{S}} |r_i| \geq \beta$, $\|\mathbf{R}\|_2, \|\Sigma\|_2, \|\mathbf{w}^*\|_2 \simeq O(1)$ and $n \gtrsim 1/\beta^2 \cdot t^2 s \cdot (\text{Tr}^{2/3}(\Sigma) + \text{Tr}(\mathbf{R}\Sigma\mathbf{R})) \cdot \text{poly}(\log(d/\delta))$. Then set $\eta \lesssim 1/\|\mathbf{R}\Sigma\mathbf{R}\|_2$ and $\eta t \simeq \frac{1}{\beta} \cdot \left(\frac{\sigma^2 \text{Tr}(\mathbf{R}\Sigma\mathbf{R}) \log(d/\delta)}{n} + \frac{\sigma^2 s \text{Tr}(\Sigma) \log^2(d/\delta)}{n^2} \right)^{-1/2}$, it holds that

$$\mathcal{E}(\tilde{\mathbf{w}}_{\text{gd}}^t) \lesssim \frac{\log t}{\beta} \sqrt{\frac{\sigma^2 \text{Tr}(\mathbf{R}\Sigma\mathbf{R}) \log(d/\delta)}{n} + \frac{\sigma^2 s \text{Tr}(\Sigma) \log^2(d/\delta)}{n^2}},$$

with probability at least $1 - \delta$.

Theorem E.1 provides an upper bound on the excess risk achieved by the preprocess-then-optimize algorithm, where we tuned learning rate η to balance the bias and variance error. Then, it can be seen that the risk bound is valid if $\text{Tr}(\mathbf{R}\Sigma\mathbf{R})/n \rightarrow 0$ and $\text{Tr}(\Sigma)s/n^2 \rightarrow 0$ when $n \rightarrow \infty$. This can be readily satisfied if we have $\|\mathbf{w}^*\|_2$ and $\text{Tr}(\Sigma)$ be bounded by some reasonable quantities that are independent of the sample size n , which are the common assumptions made in many prior works (Zou et al., 2022; 2021; Bartlett et al., 2020). Besides, it can be also seen that the excess risk bound explicitly depends on the sparsity parameter s and lower sparsity implies better performance. This implies the ability of the proposed preprocess-then-optimize for discovering and leveraging the nice sparse structure of the ground truth.

As a comparison, the following theorem states the excess risk bound for the standard gradient descents on the raw features. To make a fair comparison, we consider using the same number of steps but allow the step size to be tuned separately.

550 **Theorem B.2.** Suppose that $\|\Sigma\|, \|\mathbf{w}^*\|_2 \simeq O(1)$ and $n \gtrsim t^2(\text{Tr}(\Sigma) + \log(1/\delta))$. When $\eta \lesssim 1/\|\Sigma\|_2$ and $\eta t \simeq$
 551 $\left(\frac{\sigma^2 \text{Tr}(\Sigma) \log(d/\delta)}{n}\right)^{-1/2}$, it holds that

$$552 \mathcal{E}(\mathbf{w}_{\text{gd}}^t) \lesssim \log t \cdot \sqrt{\frac{\sigma^2 \text{Tr}(\Sigma) \log(d/\delta)}{n}},$$

553
 554 with probability at least $1 - \delta$.
 555

556 We are now able to make a rough comparison between the excess risk bounds in Theorems E.1 and E.2. Then, it is clear that
 557 $\mathcal{E}(\tilde{\mathbf{w}}_{\text{gd}}^t) \lesssim \mathcal{E}(\mathbf{w}_{\text{gd}}^t)$ requires $\text{Tr}(\mathbf{R}\Sigma\mathbf{R})/\beta^2 \lesssim \text{Tr}(\Sigma)$ and $s/(n^2\beta^2) \leq 1/n$. Specifically, we can consider the case that Σ to
 558 be a diagonal matrix, assume $w_i^* \sim \mathcal{U}\{-1/\sqrt{s}, 1/\sqrt{s}\}$ has a restricted uniform prior for $i \in \mathcal{S}$ and $\min_{i \in \mathcal{S}} \Sigma_{ii} \geq 1/\kappa$ for
 559 some constant $\kappa > 1$, we can get $\beta \geq \sqrt{1/(s\kappa^2)}$, thus $\text{Tr}(\mathbf{R}\Sigma\mathbf{R})/\beta^2 \leq \kappa^2 \sum_{i:w_i^* \neq 0} \Sigma_{ii}$ and $s/(n^2\beta^2) \leq \kappa^2 s^2/n^2$. Note
 560 that $|\mathcal{S}| = s \ll d$, then if the covariance matrix Σ has a flat eigenspectrum such that $\sum_{i \in \mathcal{S}} \Sigma_{ii} \ll \sum_{i \in [d]} \Sigma_{ii} = \text{Tr}(\Sigma)$,
 561 we have $\text{Tr}(\mathbf{R}\Sigma\mathbf{R})/\beta^2 \leq \text{Tr}(\Sigma)$ and $s/(n^2\beta^2) \leq \kappa^2 s^2/n$ if $s = o(\min\{d, \sqrt{n}\})$. This suggests that the preprocess-then-
 562 optimization algorithm can outperform the standard gradient descent for solving a sparse linear regression problem with
 563 $s = o(\min\{d, \sqrt{n}\})$.
 564

565 To make a more rigorous comparison, we next consider the example where $x_i \stackrel{\text{i.i.d.}}{\sim} \mathcal{N}(\mathbf{0}, \mathbf{I})$, based on which we can get the
 566 upper bound for our algorithm and the lower bound for OLS, ridge regression, and finite-step GD.
 567

568 **Theorem B.3** (Theorem 5.1, restated). Suppose \mathcal{S} with $|\mathcal{S}| = s$ is selected such that each element is chosen with equal
 569 probability from the set $\{1, 2, \dots, d\}$ and $w_i^* \sim \mathcal{U}\{-1/\sqrt{s}, 1/\sqrt{s}\}$ has a restricted uniform prior for $i \in \mathcal{S}$, $\|\mathbf{w}^*\|_2 \simeq \Theta(1)$
 570 and $n \gtrsim t^2 s^3 d^{2/3}$. Then there exists a choice of η and t such that

$$571 \mathcal{E}(\tilde{\mathbf{w}}_{\text{gd}}^t) \lesssim \sigma^2 \log^2(ns/\sigma^2) \log^2(d/\delta) \cdot \left(\frac{s}{n} + \frac{ds^2}{n^2}\right),$$

572 with probability at least $1 - \delta$. Besides, let $\hat{\mathbf{w}}_\lambda$ be the ridge regression estimator with regularized parameter λ , and \mathbf{w}_{ols} be
 573 the OLS estimator, it holds that

$$574 \mathbb{E}_{\mathbf{w}^*}[\mathcal{E}(\mathbf{w})] \gtrsim \begin{cases} \frac{\sigma^2 d}{n} & n \gtrsim d + \log(1/\delta) \\ 1 - \frac{n}{d} + \frac{\sigma^2 n}{d} & d \gtrsim n + \log(1/\delta), \end{cases}$$

575 with probability at least $1 - \delta$, where $\mathbf{w} \in \{\hat{\mathbf{w}}_\lambda, \mathbf{w}_{\text{ols}}, \mathbf{w}_{\text{gd}}^t\}$.
 576

577 C. Additional Details for Section 4

578 C.1. Details and Explanations of Preprocessing-then-Optimizing Algorithm

579 We note that (Guo et al., 2023) adapts a similar two-phase idea to explain how transformer learning specific functions in
 580 context, in their constructed transformers, the first few layers utilize MLPs to compute an appropriate representation for each
 581 entry, while the subsequent layers utilize the attention module to implement gradient descent over the context. We highlight
 582 that our algorithm mainly focus on utilizing multihead attention, and it aligns well with the our experimental observation
 583 and intuition. The details of our algorithm are as follows:
 584

585 **Preprocessing on In-context Examples** We summarize this procedure in Alg. 1, we highlight that the preprocessing
 586 procedure aligns well with the structure of a multi-head attention layer with linear attention, which motivates our theo-
 587 retical construction of the desired transformer. In particular, each head of the attention layer can be conceptualized as
 588 executing specific operations on a distinct subset of data entries. Then, the linear query-key calculation, represented as
 589 $(\mathbf{W}_{K_i} \mathbf{H})^\top \mathbf{W}_{Q_i} \mathbf{H}$, where $\mathbf{H} = \mathbf{E}$ denotes the input sequence embedding matrix, effectively estimates correlations between
 590 the i -th subset of data entries and the corresponding label y_i . Here, \mathbf{W}_{K_i} and \mathbf{W}_{Q_i} selectively extract entries from the i -th
 591 subset of features and the label, respectively, akin to an "entries selection" process. Furthermore, when combined with the
 592 value calculation $\mathbf{W}_{V_i} \mathbf{H}$, each head of the attention layer conducts correlation calculations for the i -th subset of features and
 593 subsequently employs them to reweight the original features within the same subset. Consequently, by stacking the outputs
 594

of multiple heads, all data features can be reweighted accordingly, which matches the design of the proposed preprocessing procedure in Alg. 1. We formally prove this in the following theorem.

Proposition C.1 (Single-layer multi-head transformer implements Alg. 1). *There exists a single-layer transformer function TF_1 , with d heads and $d_{\text{hid}} = 3d$ hidden dimension, together with an input embedding layer with weight $\mathbf{W}_E \in \mathbb{R}^{d_{\text{hid}} \times d}$, that can implement Alg. 1. Let \mathbf{E} be the input sequence defined in Eq.(2.2) and $\tilde{\mathbf{x}}_i = \hat{\mathbf{R}}\mathbf{x}$ be the preprocessed features defined in Alg. 1, it holds that*

$$\mathbf{H}^{(1)} := \text{TF}_1 \circ \mathbf{W}_E(\mathbf{E}) = \begin{pmatrix} \tilde{\mathbf{x}}_1 & \tilde{\mathbf{x}}_2 & \cdots & \tilde{\mathbf{x}}_n & \tilde{\mathbf{x}}_{n+1} & \cdots & \tilde{\mathbf{x}}_{n+q} \\ y_1 & y_2 & \cdots & y_n & 0 & \cdots & 0 \\ \vdots & \vdots & \ddots & \vdots & \vdots & \ddots & \vdots \end{pmatrix}, \quad (\text{C.1})$$

where \cdots in third row implies arbitrary values.

Optimizing Over Preprocessed In-Context Examples To maintain clarity in our construction and explanation, in each layer, we use a linear projection $\mathbf{W}_1^{(i)}$ to rearrange the dimensions of the sequence processed by the multi-head attention, resulting in the hidden state $\mathbf{H}^{(i)}$ of each layer. We refer to the first d rows of the input data as \mathbf{x} , and the $(d+1)$ -th row as the corresponding y . For example, in Eq.(C.1), we take the first d rows, together with the $(d+1)$ -th row, as the input data entry $\{\tilde{\mathbf{x}}_i, y_i\}_{i=1}^{n+1}$. Then, the following proposition shows that the subsequent layers of transformer can implement multi-step gradient descent on the preprocessed in-context examples $\{\tilde{\mathbf{x}}_i, y_i\}_{i=1, \dots, n}$.

Proposition C.2 (Subsequent single-head transformer implements multi-step GD). *There exists a transformer with k layers, 1 head, $d_{\text{hid}} = 3d$, let \hat{y}_{n+1}^ℓ be the prediction representation of the ℓ -th layer, then it holds that $\hat{y}_{n+1}^\ell = \langle \mathbf{w}_{\text{gd}}^\ell, \tilde{\mathbf{x}}_{n+1} \rangle$, where $\tilde{\mathbf{x}}_{n+1} = \hat{\mathbf{R}}\mathbf{x}_{n+1}$ denotes the preprocessed data feature, $\mathbf{w}_{\text{gd}}^\ell$ is defined as $\mathbf{w}_{\text{gd}}^0 = 0$ and as follows for $\ell = 0, \dots, k-1$:*

$$\mathbf{w}_{\text{gd}}^{\ell+1} = \mathbf{w}_{\text{gd}}^\ell - \eta \nabla \tilde{L}(\mathbf{w}_{\text{gd}}^\ell), \quad \text{where} \quad \tilde{L}(\mathbf{w}) = \frac{1}{2n} \sum_{i=1}^n (y_i - \langle \mathbf{w}, \tilde{\mathbf{x}}_i \rangle)^2. \quad (\text{C.2})$$

C.2. Proof for Proposition C.1

Proposition C.3 (Restate of Proposition C.1). *There exists a transformer with 1 layers, $h = d$ heads, $d_{\text{hid}} = 3d$ and the input projection $\mathbf{W}_E \in \mathbb{R}^{(d+1) \times d_{\text{hid}}}$ such that with the input sequence \mathbf{E} set as Equation 2.2 the first attention layer can implement Algorithm 1 so that each of the enhanced data $\{\hat{r}_i \mathbf{x}_{i,j}\}_{i \in [d]}$ can be found in the output representation $\mathbf{H}^{(1)}$:*

$$\mathbf{H}^{(1)} = \text{TF}_1 \circ \mathbf{W}_E(\mathbf{E}) = \begin{pmatrix} \tilde{\mathbf{x}}_1 & \tilde{\mathbf{x}}_2 & \cdots & \tilde{\mathbf{x}}_n & \tilde{\mathbf{x}}_{n+1} & \cdots & \tilde{\mathbf{x}}_{n+q} \\ y_1 & y_2 & \cdots & y_n & 0 & \cdots & 0 \\ \vdots & \vdots & \ddots & \vdots & \vdots & \ddots & \vdots \end{pmatrix}.$$

Proof. Here we first explain the key steps of our constructed transformer: the model first rearrange the input entries with a input projection to divide the input data into d subspace \mathbf{W}_E , each subspace includes an entry of \mathbf{x} and the corresponding y (step C.4), then use h parameters $\{\mathbf{W}_{V_i}, \mathbf{W}_{K_i}, \mathbf{W}_{Q_i}\}_{i=1}^h$ to calculate h queries, keys and values (step C.5), and compute the attention output for each head and concatenate them together (step C.6), finally use a projection matrix \mathbf{W}_1 rearrange

the result, resulting the target output (step C.7):

$$\mathbf{E} = \begin{pmatrix} \mathbf{x}_1 & \mathbf{x}_2 & \cdots & \mathbf{x}_n & \mathbf{x}_{n+1} & \cdots & \mathbf{x}_{n+q} \\ y_1 & y_2 & \cdots & y_n & 0 & \cdots & 0 \end{pmatrix} \quad (\text{C.3})$$

$$\begin{array}{l} \text{input projection} \\ \mathbf{W}_E \in \mathbb{R}^{(d+1) \times d_{\text{hid}}} \end{array} \rightarrow \mathbf{H} = \begin{pmatrix} \mathbf{x}_{1,1} & \mathbf{x}_{2,1} & \cdots & \mathbf{x}_{n,1} & \mathbf{x}_{(n+1),1} & \cdots & \mathbf{x}_{(n+q),1} \\ y_1 & y_2 & \cdots & y_n & 0 & \cdots & 0 \\ 0 & 0 & \cdots & 0 & 0 & \cdots & 0 \\ \vdots & \vdots & \ddots & \vdots & \vdots & \ddots & \vdots \end{pmatrix} \quad (\text{C.4})$$

$$\begin{array}{l} \text{compute } \mathbf{Q}_i, \mathbf{K}_i, \mathbf{V}_i \\ \mathbf{W}_{V_i}, \mathbf{W}_{K_i}, \mathbf{W}_{Q_i} \in \mathbb{R}^{3 \times d_{\text{hid}}} \end{array} \rightarrow \mathbf{K}_i = \frac{1}{n} \begin{pmatrix} 0 & \cdots & 0 & 0 & \cdots \\ 0 & \cdots & 0 & 0 & \cdots \\ y_1 & \cdots & y_n & 0 & \cdots \end{pmatrix}; \mathbf{Q}_i, \mathbf{V}_i = \begin{pmatrix} 0 & \cdots & 0 & 0 & \cdots \\ 0 & \cdots & 0 & 0 & \cdots \\ \mathbf{x}_{1,i} & \cdots & \mathbf{x}_{n,i} & \mathbf{x}_{(n+1),i} & \cdots \end{pmatrix} \quad (\text{C.5})$$

$$\begin{array}{l} \text{Attn}(\mathbf{W}_E(\mathbf{E})) \\ \mathbf{H} + \text{Concat}\{\mathbf{V}_i \mathbf{M} \mathbf{K}_i^\top \mathbf{Q}_i\} \end{array} \rightarrow \begin{pmatrix} \mathbf{x}_{1,1} & \mathbf{x}_{2,1} & \cdots & \mathbf{x}_{n,1} & \mathbf{x}_{(n+1),1} & \cdots & \mathbf{x}_{(n+q),1} \\ y_1 & y_2 & \cdots & y_n & 0 & \cdots & 0 \\ \tilde{\mathbf{x}}_{1,1} & \tilde{\mathbf{x}}_{2,1} & \cdots & \tilde{\mathbf{x}}_{n,1} & \tilde{\mathbf{x}}_{(n+1),1} & \cdots & \tilde{\mathbf{x}}_{(n+q),1} \\ \vdots & \vdots & \ddots & \vdots & \vdots & \ddots & \vdots \end{pmatrix} \quad (\text{C.6})$$

$$\begin{array}{l} \mathbf{H}^{(1)} = \text{TF}_1 \circ \mathbf{W}_E(\mathbf{E}) \\ \mathbf{W}_1 \in \mathbb{R}^{d_{\text{hid}} \times d_{\text{hid}}} \end{array} \rightarrow \begin{pmatrix} \tilde{\mathbf{x}}_1 & \tilde{\mathbf{x}}_2 & \cdots & \tilde{\mathbf{x}}_n & \tilde{\mathbf{x}}_{n+1} & \cdots & \tilde{\mathbf{x}}_{n+q} \\ y_1 & y_2 & \cdots & y_n & 0 & \cdots & 0 \\ \vdots & \vdots & \ddots & \vdots & \vdots & \ddots & \vdots \end{pmatrix} \quad (\text{C.7})$$

. The detailed parameters and calculation process for each step are as follows:

- we set $\mathbf{W}_E \in \mathbb{R}^{(d+1) \times d_{\text{hid}}}$ to rearrange the entries:

$$\mathbf{W}_E = \begin{pmatrix} \mathbb{1}[1] & \mathbb{1}[d+1] & \mathbf{0} & \mathbb{1}[2] & \mathbb{1}[d+1] & \mathbf{0} & \cdots & \mathbb{1}[d] & \mathbb{1}[d+1] & \mathbf{0} \end{pmatrix}^\top,$$

where $\mathbb{1}[k]$ is an $1 \times d_{\text{hid}}$ vector with 1 at i -th entry and 0 elsewhere, such that

$$\mathbf{H} = \mathbf{W}_E \mathbf{E} = \begin{pmatrix} \mathbf{x}_{1,1} & \mathbf{x}_{2,1} & \cdots & \mathbf{x}_{n,1} & \mathbf{x}_{(n+1),1} & \cdots & \mathbf{x}_{(n+q),1} \\ y_1 & y_2 & \cdots & y_n & 0 & \cdots & 0 \\ 0 & 0 & \cdots & 0 & 0 & \cdots & 0 \\ \mathbf{x}_{1,2} & \mathbf{x}_{2,2} & \cdots & \mathbf{x}_{n,2} & \mathbf{x}_{(n+1),2} & \cdots & \mathbf{x}_{(n+q),2} \\ \vdots & \vdots & \ddots & \vdots & \vdots & \ddots & \vdots \end{pmatrix}.$$

- we set $\mathbf{W}_{V_i}, \mathbf{W}_{K_i}, \mathbf{W}_{Q_i} \in \mathbb{R}^{3 \times d_{\text{hid}}}$ for values, keys and queries:

$$\mathbf{W}_{K_i} = \frac{1}{n} \begin{pmatrix} \mathbf{0} \\ \mathbf{0} \\ \mathbb{1}[3i-1] \end{pmatrix}; \quad \mathbf{W}_{V_i}, \mathbf{W}_{Q_i} = \begin{pmatrix} \mathbf{0} \\ \mathbf{0} \\ \mathbb{1}[3i-2] \end{pmatrix},$$

such that the i -th head extract i -th entry of \mathbf{x} and corresponding y

$$\mathbf{K}_i = \frac{1}{n} \begin{pmatrix} \mathbf{0} \\ \mathbf{0} \\ \mathbb{1}[3i-1] \end{pmatrix} \begin{pmatrix} \mathbf{x}_{1,1} & \mathbf{x}_{2,1} & \cdots & \mathbf{x}_{n,1} & \mathbf{x}_{(n+1),1} & \cdots \\ y_1 & y_2 & \cdots & y_n & 0 & \cdots \\ 0 & 0 & \cdots & 0 & 0 & \cdots \\ \mathbf{x}_{1,2} & \mathbf{x}_{2,2} & \cdots & \mathbf{x}_{n,2} & \mathbf{x}_{(n+1),2} & \cdots \\ \vdots & \vdots & \ddots & \vdots & \vdots & \ddots \end{pmatrix} = \frac{1}{n} \begin{pmatrix} 0 & \cdots & 0 & 0 & \cdots \\ 0 & \cdots & 0 & 0 & \cdots \\ y_1 & \cdots & y_n & 0 & \cdots \end{pmatrix},$$

$$\mathbf{Q}_i, \mathbf{V}_i = \begin{pmatrix} \mathbf{0} \\ \mathbf{0} \\ \mathbb{1}[3i-2] \end{pmatrix} \begin{pmatrix} \mathbf{x}_{1,1} & \mathbf{x}_{2,1} & \cdots & \mathbf{x}_{n,1} & \mathbf{x}_{(n+1),1} & \cdots \\ y_1 & y_2 & \cdots & y_n & 0 & \cdots \\ 0 & 0 & \cdots & 0 & 0 & \cdots \\ \mathbf{x}_{1,2} & \mathbf{x}_{2,2} & \cdots & \mathbf{x}_{n,2} & \mathbf{x}_{(n+1),2} & \cdots \\ \vdots & \vdots & \ddots & \vdots & \vdots & \ddots \end{pmatrix} = \begin{pmatrix} 0 & \cdots & 0 & 0 & \cdots \\ 0 & \cdots & 0 & 0 & \cdots \\ \mathbf{x}_{1,i} & \cdots & \mathbf{x}_{n,i} & \mathbf{x}_{(n+1),i} & \cdots \end{pmatrix},$$

$$\begin{aligned}
 \mathbf{V}_i \mathbf{M} \mathbf{K}_i^\top \mathbf{Q}_i &= \begin{pmatrix} 0 & \cdots & 0 & 0 & \cdots & 0 \\ 0 & \cdots & 0 & 0 & \cdots & 0 \\ \mathbf{x}_{1,i} & \cdots & \mathbf{x}_{n,i} & \mathbf{x}_{(n+1),i} & \cdots & \mathbf{x}_{(n+q),i} \end{pmatrix} \begin{pmatrix} \mathbf{I}_n & \mathbf{0} \\ \mathbf{0} & \mathbf{0} \end{pmatrix}. \\
 &= \begin{pmatrix} 0 & \cdots & 0 & 0 & \cdots & 0 \\ 0 & \cdots & 0 & 0 & \cdots & 0 \\ y_1 & \cdots & y_n & 0 & \cdots & 0 \end{pmatrix}^\top \begin{pmatrix} 0 & \cdots & 0 & 0 & \cdots & 0 \\ 0 & \cdots & 0 & 0 & \cdots & 0 \\ \mathbf{x}_{1,i} & \cdots & \mathbf{x}_{n,i} & \mathbf{x}_{(n+1),i} & \cdots & \mathbf{x}_{(n+q),i} \end{pmatrix} \\
 &= \begin{pmatrix} 0 & \cdots & 0 & 0 & \cdots & 0 \\ 0 & \cdots & 0 & 0 & \cdots & 0 \\ \tilde{\mathbf{x}}_{1,i} & \cdots & \tilde{\mathbf{x}}_{n,i} & \tilde{\mathbf{x}}_{(n+1),i} & \cdots & \tilde{\mathbf{x}}_{(n+q),i} \end{pmatrix}.
 \end{aligned}$$

- Then concatenate the output of each head $\{\mathbf{V}_i \mathbf{M} \mathbf{K}_i^\top \mathbf{Q}_i\}_{i=1}^h$ together with residue:

$$\mathbf{H} + \text{Concat}[\{\mathbf{V}_i \mathbf{M} \mathbf{K}_i^\top \mathbf{Q}_i\}_{i=1}^h] = \begin{pmatrix} \mathbf{x}_{1,1} & \mathbf{x}_{2,1} & \cdots & \mathbf{x}_{n,1} & \mathbf{x}_{(n+1),1} & \cdots & \mathbf{x}_{(n+q),1} \\ y_1 & y_2 & \cdots & y_n & 0 & \cdots & 0 \\ \tilde{\mathbf{x}}_{1,1} & \tilde{\mathbf{x}}_{2,1} & \cdots & \tilde{\mathbf{x}}_{n,1} & \tilde{\mathbf{x}}_{(n+1),1} & \cdots & \tilde{\mathbf{x}}_{(n+q),1} \\ \vdots & \vdots & \ddots & \vdots & \vdots & \ddots & \vdots \end{pmatrix}. \quad (\text{C.8})$$

- Finally, \mathbf{W}_1 is applied to rearrange the entries:

$$\mathbf{W}_1 = \begin{pmatrix} \mathbb{1}[3] & \cdots & \mathbb{1}[3d] & \mathbb{1}[2] & \cdots \end{pmatrix}^\top,$$

where the first \cdots implies the omitted $d-2$ vectors $\{\mathbb{1}[3i] | i = 2, 3, \dots, (d-1)\}$, the second \cdots implies arbitrary values, then resulting the final output:

$$\mathbf{H}^{(1)} = \mathbf{W}_1 [\mathbf{H} + \text{Concat}[\{\mathbf{V}_i \mathbf{M} \mathbf{K}_i^\top \mathbf{Q}_i\}_{i=1}^h]] = \begin{pmatrix} \tilde{\mathbf{x}}_1 & \tilde{\mathbf{x}}_2 & \cdots & \tilde{\mathbf{x}}_n & \tilde{\mathbf{x}}_{n+1} & \cdots & \tilde{\mathbf{x}}_{n+q} \\ y_1 & y_2 & \cdots & y_n & 0 & \cdots & 0 \\ \vdots & \vdots & \ddots & \vdots & \vdots & \ddots & \vdots \end{pmatrix}.$$

in this way we construct a transformer that can apply Alg. 1 so that each of the enhanced data $\{\hat{r}_i \mathbf{x}_{i,j}\}_{i \in [d]}$ can be found in the output representation $\mathbf{H}^{(1)}$. \square

C.3. Proof for Proposition C.2

Proposition C.4 (Restate of Proposition C.2). *There exists a transformer with k layers, 1 head, $d_{\text{hid}} = 3d$, let $\{(\tilde{\mathbf{x}}_i, \hat{y}_i^\ell)\}_{i=1}^{n+1}$ be the ℓ -th layer input data entry, then it holds that $\hat{y}_{(n+1)}^\ell = \langle \mathbf{w}_{\text{gd}}^\ell, \tilde{\mathbf{x}}_{n+1} \rangle$, where \mathbf{w}_{gd} is defined as $\mathbf{w}_{\text{gd}}^0 = \mathbf{0}$ and as follows for $\ell = 0, \dots, k-1$:*

$$\mathbf{w}_{\text{gd}}^{\ell+1} = \mathbf{w}_{\text{gd}}^\ell - \eta \nabla \tilde{L}(\mathbf{w}_{\text{gd}}^\ell), \quad \text{where} \quad \tilde{L}(\mathbf{w}) = \frac{1}{2n} \sum_{i=1}^n (y_i - \langle \mathbf{w}, \tilde{\mathbf{x}}_i \rangle)^2.$$

Proof. Here we directly provide the parameters $\mathbf{W}_V^\ell, \mathbf{W}_K^\ell, \mathbf{W}_Q^\ell \in \mathbb{R}^{d_{\text{hid}} \times d_{\text{hid}}}$ and $\mathbf{W}_1^\ell \in \mathbb{R}^{d_{\text{hid}} \times d_{\text{hid}}}$ for each layer TF_ℓ ,

$$\mathbf{W}_V^\ell = -\frac{\eta}{n} \begin{pmatrix} \mathbf{0} & \mathbf{0} \\ \mathbf{0} & \mathbf{1} \end{pmatrix}; \quad \mathbf{W}_K^\ell, \mathbf{W}_Q^\ell = \begin{pmatrix} \mathbf{I}_{d \times d} & \mathbf{0} \\ \mathbf{0} & \mathbf{0} \end{pmatrix}; \quad \mathbf{W}_1^\ell = \mathbf{I}_{d_{\text{hid}} \times d_{\text{hid}}} \quad (\text{C.9})$$

As we set \mathbf{W}_1^ℓ as the identity matrix, we can ignore it and then apply Lemma 1 in (Ahn et al.). By replacing $(\mathbf{W}_K^\ell \mathbf{W}_Q^\ell)$ as \mathbf{Q}_i and \mathbf{W}_V^ℓ with \mathbf{P}_i , then it holds that $\hat{y}_{(n+1)}^\ell = \langle \mathbf{w}_{\text{gd}}^\ell, \tilde{\mathbf{x}}_{n+1} \rangle$, where \mathbf{w}_{gd} is defined as $\mathbf{w}_{\text{gd}}^0 = \mathbf{0}$ and as follows for $\ell = 0, \dots, k-1$:

$$\mathbf{w}_{\text{gd}}^{\ell+1} = \mathbf{w}_{\text{gd}}^\ell - \eta \nabla \tilde{L}(\mathbf{w}_{\text{gd}}^\ell), \quad \text{where} \quad \tilde{L}(\mathbf{w}) = \frac{1}{2n} \sum_{i=1}^n (y_i - \langle \mathbf{w}, \tilde{\mathbf{x}}_i \rangle)^2.$$

\square

D. Additional Related Work

In addition to works towards understanding the expressive power of transformers that we introduced before, there is also a body of research on the mechanism interpretation and the training dynamics of transformers:

Mechanism interpretation of trained transformers To understand the mechanisms in trained transformers, researchers have developed various techniques, including interpreting transformers into programming languages (Friedman et al.; Lindner et al., 2023; Weiss et al., 2021; Zhou et al., 2024), probing the behavior of individual layers (Pandit & Hou, 2021; Wu et al., 2020; Bricken et al., 2023; Allen-Zhu & Li, 2023; Zhu & Li, 2023), and incorporating transformers with other large language models to interpret individual neurons (Bills et al., 2023). While these techniques provide high-level insights into transformer mechanism understanding, providing a clear algorithms behind the trained transformers is still very challenging.

Training dynamics of transformers In parallel, a body of work has also investigated how transformers learn these algorithms, i.e., the training dynamics of transformers. (Tarzanagh et al., 2023) shows an equivalence between a single attention layer and a support vector machine. (Zhang et al., 2023; Huang et al., 2023) analyze the training dynamics of a single-head attention layer for in-context linear regression, where (Zhang et al., 2023) demonstrates that it can converge to implement one-step gradient over in-context examples. Additionally, (Tian et al., 2023; Li et al., 2023) study the convergence of transformers on sequences of discrete tokens. These works provide valuable insights towards the theoretical understanding of the training dynamics of transformers, which offer potential future extension aspects for our work.

E. Theoretical Analysis of the Preprocess-then-optimize Algorithm

E.1. Notations

For two functions $f(x) \geq 0$ and $g(x) \geq 0$ defined on the positive real numbers ($x > 0$), we write $f(x) \lesssim g(x)$ if there exists two constants $c, x_0 > 0$ such that $\forall x \geq x_0, f(x) \leq c \cdot g(x)$; we write $f(x) \gtrsim g(x)$ if $g(x) \lesssim f(x)$; we write $f(x) \asymp g(x)$ if $f(x) \lesssim g(x)$ and $g(x) \lesssim f(x)$. If $f(x) \lesssim g(x)$, we can write $f(x)$ as $O(g(x))$. We can also write $f(x)$ as $\tilde{O}(g(x))$ if there exists a constant $k > 0$ such that $f(x) \lesssim g(x) \log^k(x)$.

E.2. Theoretical results

We first provide the upper bound of the excess risk for $\mathcal{E}(\tilde{\mathbf{w}}_{\text{gd}}^t)$ and $\mathcal{E}(\mathbf{w}_{\text{gd}}^t)$ respectively.

Theorem E.1. Denote $\mathcal{S} := \{i : w_i^* \neq 0\}$ and $\mathbf{R} = \text{diag}\{r_1, \dots, r_d\}$, where $r_j = \sum_{i=1}^d w_i^* \Sigma_{ij}$. Suppose that there exist a $\beta > 0$ such that $\min_{i \in \mathcal{S}} |r_i| \geq \beta$, $\|\mathbf{R}\|_2, \|\Sigma\|_2, \|\mathbf{w}^*\|_2 \simeq O(1)$ and $n \gtrsim 1/\beta^2 \cdot t^2 s \cdot (\text{Tr}^{2/3}(\Sigma) + \text{Tr}(\mathbf{R}\Sigma\mathbf{R})) \cdot \text{poly}(\log(d/\delta))$. Then set $\eta \lesssim 1/\|\mathbf{R}\Sigma\mathbf{R}\|_2$ and $\eta t \simeq \frac{1}{\beta} \cdot \left(\frac{\sigma^2 \text{Tr}(\mathbf{R}\Sigma\mathbf{R}) \log(d/\delta)}{n} + \frac{\sigma^2 s \text{Tr}(\Sigma) \log^2(d/\delta)}{n^2} \right)^{-1/2}$, it holds that

$$\mathcal{E}(\tilde{\mathbf{w}}_{\text{gd}}^t) \lesssim \frac{\log t}{\beta} \sqrt{\frac{\sigma^2 \text{Tr}(\mathbf{R}\Sigma\mathbf{R}) \log(d/\delta)}{n} + \frac{\sigma^2 s \text{Tr}(\Sigma) \log^2(d/\delta)}{n^2}},$$

with probability at least $1 - \delta$.

Theorem E.1 provides an upper bound on the excess risk achieved by the preprocess-then-optimize algorithm, where we tuned learning rate η to balance the bias and variance error. Then, it can be seen that the risk bound is valid if $\text{Tr}(\mathbf{R}\Sigma\mathbf{R})/n \rightarrow 0$ and $\text{Tr}(\Sigma)s/n^2 \rightarrow 0$ when $n \rightarrow \infty$. This can be readily satisfied if we have $\|\mathbf{w}^*\|_2$ and $\text{Tr}(\Sigma)$ be bounded by some reasonable quantities that are independent of the sample size n , which are the common assumptions made in many prior works (Zou et al., 2022; 2021; Bartlett et al., 2020). Besides, it can be also seen that the excess risk bound explicitly depends on the sparsity parameter s and lower sparsity implies better performance. This implies the ability of the proposed preprocess-then-optimize for discovering and leveraging the nice sparse structure of the ground truth.

As a comparison, the following theorem states the excess risk bound for the standard gradient descents on the raw features. To make a fair comparison, we consider using the same number of steps but allow the step size to be tuned separately.

Theorem E.2. Suppose that $\|\Sigma\|, \|\mathbf{w}^*\|_2 \simeq O(1)$ and $n \gtrsim t^2(\text{Tr}(\Sigma) + \log(1/\delta))$. When $\eta \lesssim 1/\|\Sigma\|_2$ and $\eta t \simeq$

825 $\left(\frac{\sigma^2 \text{Tr}(\boldsymbol{\Sigma}) \log(d/\delta)}{n}\right)^{-1/2}$, it holds that

$$826 \quad 827 \quad 828 \quad 829 \quad \mathcal{E}(\mathbf{w}_{\text{gd}}^t) \lesssim \log t \cdot \sqrt{\frac{\sigma^2 \text{Tr}(\boldsymbol{\Sigma}) \log(d/\delta)}{n}},$$

830 with probability at least $1 - \delta$.

831
832 We are now able to make a rough comparison between the excess risk bounds in Theorems E.1 and E.2. Then, it is clear that
833 $\mathcal{E}(\tilde{\mathbf{w}}_{\text{gd}}^t) \lesssim \mathcal{E}(\mathbf{w}_{\text{gd}}^t)$ requires $\text{Tr}(\mathbf{R}\boldsymbol{\Sigma}\mathbf{R})/\beta^2 \lesssim \text{Tr}(\boldsymbol{\Sigma})$ and $s/(n^2\beta^2) \leq 1/n$. Specifically, we can consider the case that $\boldsymbol{\Sigma}$ to
834 be a diagonal matrix, assume $w_i^* \sim \mathcal{U}\{-1/\sqrt{s}, 1/\sqrt{s}\}$ has a restricted uniform prior for $i \in \mathcal{S}$ and $\min_{i \in \mathcal{S}} \Sigma_{ii} \geq 1/\kappa$ for
835 some constant $\kappa > 1$, we can get $\beta \geq \sqrt{1/(s\kappa^2)}$, thus $\text{Tr}(\mathbf{R}\boldsymbol{\Sigma}\mathbf{R})/\beta^2 \leq \kappa^2 \sum_{i: w_i^* \neq 0} \Sigma_{ii}$ and $s/(n^2\beta^2) \leq \kappa^2 s^2/n^2$. Note
836 that $|\mathcal{S}| = s \ll d$, then if the covariance matrix $\boldsymbol{\Sigma}$ has a flat eigenspectrum such that $\sum_{i \in \mathcal{S}} \Sigma_{ii} \ll \sum_{i \in [d]} \Sigma_{ii} = \text{Tr}(\boldsymbol{\Sigma})$,
837 we have $\text{Tr}(\mathbf{R}\boldsymbol{\Sigma}\mathbf{R})/\beta^2 \leq \text{Tr}(\boldsymbol{\Sigma})$ and $s/(n^2\beta^2) \leq \kappa^2 s^2/n$ if $s = o(\min\{d, \sqrt{n}\})$. This suggests that the preprocess-then-
838 optimization algorithm can outperform the standard gradient descent for solving a sparse linear regression problem with
839 $s = o(\min\{d, \sqrt{n}\})$.

840
841 To make a more rigorous comparison, we next consider the example where $x_i \stackrel{\text{i.i.d.}}{\sim} \mathcal{N}(\mathbf{0}, \mathbf{I})$, based on which we can get the
842 upper bound for our algorithm and the lower bound for OLS, ridge regression, and finite-step GD.

843
844 **Theorem E.3** (Theorem 5.1, restated). Suppose \mathcal{S} with $|\mathcal{S}| = s$ is selected such that each element is chosen with equal
845 probability from the set $\{1, 2, \dots, d\}$ and $w_i^* \sim \mathcal{U}\{-1/\sqrt{s}, 1/\sqrt{s}\}$ has a restricted uniform prior for $i \in \mathcal{S}$, $\|\mathbf{w}^*\|_2 \simeq \Theta(1)$
846 and $n \gtrsim t^2 s^3 d^{2/3}$. Then there exists a choice of η and t such that

$$847 \quad 848 \quad 849 \quad \mathcal{E}(\tilde{\mathbf{w}}_{\text{gd}}^t) \lesssim \sigma^2 \log^2(ns/\sigma^2) \log^2(d/\delta) \cdot \left(\frac{s}{n} + \frac{ds^2}{n^2}\right),$$

850 with probability at least $1 - \delta$. Besides, let $\hat{\mathbf{w}}_\lambda$ be the ridge regression estimator with regularized parameter λ , and \mathbf{w}_{ols} be
851 the OLS estimator, it holds that

$$852 \quad 853 \quad 854 \quad 855 \quad \mathbb{E}_{\mathbf{w}^*}[\mathcal{E}(\mathbf{w})] \gtrsim \begin{cases} \frac{\sigma^2 d}{n} & n \gtrsim d + \log(1/\delta) \\ 1 - \frac{n}{d} + \frac{\sigma^2 n}{d} & d \gtrsim n + \log(1/\delta), \end{cases}$$

856 with probability at least $1 - \delta$, where $\mathbf{w} \in \{\hat{\mathbf{w}}_\lambda, \mathbf{w}_{\text{ols}}, \mathbf{w}_{\text{gd}}^t\}$.

857 F. Proof of Theorem E.1

858
859 To simplify the notations, we use $\hat{\mathbf{w}}_t$ to denote $\tilde{\mathbf{w}}_{\text{gd}}^t$. We first prove that with a high probability, there exists a $\bar{\mathbf{R}} \in \mathbb{R}^{d \times d}$
860 such that $\bar{\mathbf{R}}\hat{\mathbf{R}} = \hat{\mathbf{R}}\bar{\mathbf{R}} = \mathbf{I}_s$, where $\mathbf{I}_s = \text{diag}\{a_1, \dots, a_d\}$ with $a_j = 1_{\{j \in \mathcal{S}\}}$.

861
862 **Lemma F.1.** Denote $\mathbf{R} = \text{diag}\{r_1, \dots, r_d\}$, where $r_j = \sum_{i=1}^d w_i^* \Sigma_{ij}$. Suppose $n \geq \mathcal{O}(\log(d/\delta))$, then for any $\delta \in (0, 1)$
863 with probability at least $1 - \delta$, we have

$$864 \quad 865 \quad 866 \quad 867 \quad \|\hat{\mathbf{R}} - \mathbf{R}\|_2 \lesssim K \cdot \sqrt{\frac{s \log(d/\delta)}{n}},$$

868 where $K := C(\max_i \Sigma_{ii} + \sigma^2)$, where C is an absolute constant.

869
870 **Lemma F.2.** Define the event \mathcal{E}_R by $\mathcal{E}_R = \{|\hat{r}_i| \geq \frac{1}{2}|r_i|, \forall i \in \mathcal{S}\}$. Suppose that $n \gtrsim s \log(d/\delta)/\beta^2$, then $\mathbb{P}(\mathcal{E}_1) \geq 1 - \delta$.

871 We define $\bar{\mathbf{R}}$ by $\bar{\mathbf{R}} = \text{diag}\{\bar{r}_1, \dots, \bar{r}_d\}$, where \bar{r}_j is given by

$$872 \quad 873 \quad 874 \quad 875 \quad \bar{r}_j = \begin{cases} 0 & j \notin \mathcal{S}, \\ 1/\hat{r}_j & j \in \mathcal{S}. \end{cases}$$

876 It is easy to see $\bar{\mathbf{R}}\hat{\mathbf{R}} = \hat{\mathbf{R}}\bar{\mathbf{R}} = \mathbf{I}_s$. On the event \mathcal{E}_1 , we have that $\|\bar{\mathbf{R}}\| \lesssim 1/\beta$. Hereafter, we condition on \mathcal{E}_1 .

F.1. Bias-variance Decomposition

Let $\tilde{\mathbf{X}} = \mathbf{X}\hat{\mathbf{R}}$ with $\tilde{\mathbf{x}}_i = \hat{\mathbf{R}}\mathbf{x}_i$. For $\hat{\mathbf{w}}_t$, we have

$$\begin{aligned} \hat{\mathbf{w}}_{t+1} - \bar{\mathbf{R}}\mathbf{w}^* &= \hat{\mathbf{w}}_t - \bar{\mathbf{R}}\mathbf{w}^* - \eta \cdot \frac{1}{n} \sum_{i=1}^n \tilde{\mathbf{x}}_i (\tilde{\mathbf{x}}_i^\top \hat{\mathbf{w}}_t - y_i) \\ &= \hat{\mathbf{w}}_t - \bar{\mathbf{R}}\mathbf{w}^* - \eta \cdot \frac{1}{n} \sum_{i=1}^n \tilde{\mathbf{x}}_i (\tilde{\mathbf{x}}_i^\top \hat{\mathbf{w}}_t - \tilde{\mathbf{x}}_i^\top \bar{\mathbf{R}}\mathbf{w}^* + \epsilon) \\ &= (\mathbf{I} - \eta \hat{\Sigma}) (\hat{\mathbf{w}}_t - \bar{\mathbf{R}}\mathbf{w}^*) + \eta \cdot \frac{1}{n} \tilde{\mathbf{X}}^\top \epsilon. \end{aligned}$$

Hence, we have

$$\hat{\mathbf{w}}_t = \left(\mathbf{I} - (\mathbf{I} - \eta \hat{\Sigma})^t \right) \bar{\mathbf{R}}\mathbf{w}^* + \frac{1}{n} \sum_{i=1}^t (\mathbf{I} - \eta \hat{\Sigma})^{i-1} \tilde{\mathbf{X}}^\top \epsilon. \quad (\text{F.1})$$

We can decompose the risk $L(\hat{\mathbf{w}}_t)$ by

$$\mathcal{E}(\hat{\mathbf{w}}_t) = \mathbb{E}_{(\mathbf{x}, y) \sim \mathcal{P}} \left[\left(\langle \hat{\mathbf{R}}\mathbf{x}, \hat{\mathbf{w}}_t \rangle - \langle \hat{\mathbf{R}}\mathbf{x}, \bar{\mathbf{R}}\mathbf{w}^* \rangle - \epsilon \right)^2 \right] - \sigma^2 \quad (\text{F.2})$$

$$\begin{aligned} &= \mathbb{E}_{(\mathbf{x}, y) \sim \mathcal{P}} \left[\left(\langle \hat{\mathbf{R}}\mathbf{x}, \hat{\mathbf{w}}_t \rangle - \langle \hat{\mathbf{R}}\mathbf{x}, \bar{\mathbf{R}}\mathbf{w}^* \rangle \right)^2 \right] \\ &= \left\| \Sigma^{1/2} \hat{\mathbf{R}} (\hat{\mathbf{w}}_t - \bar{\mathbf{R}}\mathbf{w}^*) \right\|_2^2 \\ &= \left\| \Sigma^{1/2} \hat{\mathbf{R}} \left(-(\mathbf{I} - \eta \hat{\Sigma})^t \bar{\mathbf{R}}\mathbf{w}^* + \eta \cdot \frac{1}{n} \sum_{i=1}^t (\mathbf{I} - \eta \hat{\Sigma})^{i-1} \tilde{\mathbf{X}}^\top \epsilon \right) \right\|_2^2 \\ &= \underbrace{\left\| \Sigma^{1/2} \hat{\mathbf{R}} (\mathbf{I} - \eta \hat{\Sigma})^t \bar{\mathbf{R}}\mathbf{w}^* \right\|_2^2}_{\text{Bias}} + \eta^2 \underbrace{\left\| \Sigma^{1/2} \hat{\mathbf{R}} \left(\frac{1}{n} \sum_{i=1}^t (\mathbf{I} - \eta \hat{\Sigma})^{i-1} \tilde{\mathbf{X}}^\top \epsilon \right) \right\|_2^2}_{\text{Variance}}. \quad (\text{F.3}) \end{aligned}$$

Next, we present some lemmas.

Lemma F.3 (Theorem 9 in Bartlett et al. (2020)). *There is an absolute constant c such that for any $\delta \in (0, 1)$ with probability at least $1 - \delta$,*

$$\|\hat{\Sigma} - \Sigma\|_2 \leq c \|\Sigma\|_2 \cdot \max \left\{ \sqrt{\frac{r(\Sigma)}{n}}, \frac{r(\Sigma)}{n}, \sqrt{\frac{\log(1/\delta)}{n}}, \frac{\log(1/\delta)}{n} \right\},$$

where $r(\Sigma) = \text{Tr}(\Sigma)/\lambda_1$.

Lemma F.4. *With probability at least $1 - \delta$, we have*

$$\|\hat{\mathbf{R}}\hat{\Sigma}\hat{\mathbf{R}} - \mathbf{R}\Sigma\mathbf{R}\|_2 \lesssim \sqrt{s} \cdot \text{poly}(\log(d/\delta)) \cdot \left(\sqrt{\frac{r(\mathbf{R}\Sigma\mathbf{R})}{n}} + \frac{\sqrt{r(\Sigma)} + r(\mathbf{R}\Sigma\mathbf{R})}{n} + \frac{r(\Sigma)}{n^{3/2}} \right).$$

As a result, when $n \gtrsim st^2 (r^{2/3}(\Sigma) + r(\mathbf{R}\Sigma\mathbf{R})) \cdot \text{poly}(\log(d/\delta))$, with probability at least $1 - \delta$, we have

$$\|\hat{\mathbf{R}}\hat{\Sigma}\hat{\mathbf{R}} - \mathbf{R}\Sigma\mathbf{R}\|_2 \leq 1/t.$$

We define the event \mathcal{E}_2 as follows:

$$\mathcal{E}_2 := \left\{ \|\mathbf{R}\Sigma\mathbf{R}\|_2 \lesssim \tilde{\alpha}(n, \delta) \leq 1/t \right\},$$

935 where

$$936 \tilde{\alpha}(n, \delta) = \sqrt{s} \cdot \text{poly}(\log(d/\delta)) \cdot \left(\sqrt{\frac{r(\mathbf{R}\Sigma\mathbf{R})}{n}} + \frac{\sqrt{r(\Sigma)} + r(\mathbf{R}\Sigma\mathbf{R})}{n} + \frac{r(\Sigma)}{n^{3/2}} \right).$$

937 By Lemma F.4, $\mathbb{P}(\mathcal{E}_2) \geq 1 - \delta$. Hereafter, we condition on $\mathcal{E}_1 \cap \mathcal{E}_2$.

942 F.2. Bounding the Bias

943 On $\mathcal{E}_1 \cap \mathcal{E}_2$, we have

$$944 \begin{aligned} \text{Bias} &= \left\| \Sigma^{1/2} \widehat{\mathbf{R}} (\mathbf{I} - \eta \widehat{\Sigma})^t \overline{\mathbf{R}} \mathbf{w}^* \right\|_2^2 \\ 945 &= \mathbf{w}^{*\top} \overline{\mathbf{R}} (\mathbf{I} - \eta \widehat{\Sigma})^t \widehat{\mathbf{R}} \Sigma \widehat{\mathbf{R}} (\mathbf{I} - \eta \widehat{\Sigma})^t \overline{\mathbf{R}} \mathbf{w}^* \\ 946 &= \underbrace{\mathbf{w}^{*\top} \overline{\mathbf{R}} (\mathbf{I} - \eta \widehat{\Sigma})^t \widehat{\mathbf{R}} (\Sigma - \widehat{\Sigma}) \widehat{\mathbf{R}} (\mathbf{I} - \eta \widehat{\Sigma})^t \overline{\mathbf{R}} \mathbf{w}^*}_I + \underbrace{\mathbf{w}^{*\top} \overline{\mathbf{R}} (\mathbf{I} - \eta \widehat{\Sigma})^t \widehat{\mathbf{R}} \widehat{\Sigma} \widehat{\mathbf{R}} (\mathbf{I} - \eta \widehat{\Sigma})^t \overline{\mathbf{R}} \mathbf{w}^*}_{\text{II}}. \end{aligned} \quad (\text{F.4})$$

947 **Lemma F.5.** On $\mathcal{E}_1 \cap \mathcal{E}_2$, we have

$$948 I \lesssim \frac{1}{t\beta^2}$$

949 and

$$950 \text{II} \lesssim \frac{1}{\eta t\beta^2}.$$

951 hold with probability at least $1 - \delta$.

952 By Lemma F.5, we obtain that with probability at least $1 - \delta$,

$$953 \text{Bias} \lesssim I + \text{II} \leq \frac{1}{t\beta^2} + \frac{1}{\eta t\beta^2} \lesssim \frac{1}{\eta t\beta^2} \quad (\text{F.5})$$

954 where the last inequality is by $\eta \lesssim 1/\|\Sigma\| \lesssim 1$.

955 F.3. Bounding the Variance

$$956 \begin{aligned} \text{Variance} &= \eta^2 \left\| \Sigma^{1/2} \widehat{\mathbf{R}} \left(\frac{1}{n} \sum_{i=1}^t (\mathbf{I} - \eta \widehat{\Sigma})^{i-1} \widetilde{\mathbf{X}}^\top \epsilon \right) \right\|_2^2 \\ 957 &= \frac{\eta^2}{n^2} \epsilon^\top \mathbf{X} \widehat{\mathbf{R}} \sum_{i=1}^t (\mathbf{I} - \eta \widehat{\Sigma})^{i-1} \widehat{\mathbf{R}} \Sigma \widehat{\mathbf{R}} \sum_{i=1}^t (\mathbf{I} - \eta \widehat{\Sigma})^{i-1} \widehat{\mathbf{R}} \mathbf{X}^\top \epsilon \\ 958 &= \underbrace{\frac{\eta^2}{n^2} \epsilon^\top \mathbf{X} \widehat{\mathbf{R}} \sum_{i=1}^t (\mathbf{I} - \eta \widehat{\Sigma})^{i-1} \widehat{\mathbf{R}} (\Sigma - \widehat{\Sigma}) \widehat{\mathbf{R}} \sum_{i=1}^t (\mathbf{I} - \eta \widehat{\Sigma})^{i-1} \widehat{\mathbf{R}} \mathbf{X}^\top \epsilon}_I \\ 959 &+ \underbrace{\frac{\eta^2}{n^2} \epsilon^\top \mathbf{X} \widehat{\mathbf{R}} \sum_{i=1}^t (\mathbf{I} - \eta \widehat{\Sigma})^{i-1} \widehat{\mathbf{R}} \widehat{\Sigma} \widehat{\mathbf{R}} \sum_{i=1}^t (\mathbf{I} - \eta \widehat{\Sigma})^{i-1} \widehat{\mathbf{R}} \mathbf{X}^\top \epsilon}_{\text{II}}. \end{aligned} \quad (\text{F.6})$$

990 **Lemma F.6.** On $\mathcal{E}_1 \cap \mathcal{E}_2$, with probability at least $1 - \delta$, we have

$$991 \quad \text{I} \lesssim \frac{\eta^2 t}{n^2} \cdot \left\| \widehat{\mathbf{R}} \mathbf{X}^\top \epsilon \right\|_2^2$$

992 and

$$993 \quad \text{II} \lesssim \frac{\eta t \log t}{n^2} \cdot \left\| \widehat{\mathbf{R}} \mathbf{X}^\top \epsilon \right\|_2^2.$$

994 By applying Lemma F.6 to Eq.(F.6), we obtain that

$$995 \quad \text{Variance} = \text{I} + \text{II} \lesssim \frac{\eta^2 t}{n^2} \cdot \left\| \widehat{\mathbf{R}} \mathbf{X}^\top \epsilon \right\|_2^2 + \frac{\eta t \log t}{n^2} \cdot \left\| \widehat{\mathbf{R}} \mathbf{X}^\top \epsilon \right\|_2^2 \lesssim \frac{\eta t \log t}{n^2} \cdot \left\| \widehat{\mathbf{R}} \mathbf{X}^\top \epsilon \right\|_2^2. \quad (\text{F.7})$$

1000 **Lemma F.7.** with probability at least $1 - \delta$, we have

$$1001 \quad \left\| \frac{1}{n} \cdot \widehat{\mathbf{R}} \mathbf{X}^\top \epsilon \right\|_2^2 \lesssim \frac{\sigma^2 \text{Tr}(\mathbf{R} \boldsymbol{\Sigma} \mathbf{R}) \log(d/\delta)}{n} + \frac{\sigma^2 s \text{Tr}(\boldsymbol{\Sigma}) \log^2(d/\delta)}{n^2}$$

1002 By applying Lemma F.7 to Eq.(F.7), we obtain that

$$1003 \quad \text{Variance} \lesssim \eta t \log t \cdot \left(\frac{\sigma^2 \text{Tr}(\mathbf{R} \boldsymbol{\Sigma} \mathbf{R}) \log(d/\delta)}{n} + \frac{\sigma^2 s \text{Tr}(\boldsymbol{\Sigma}) \log^2(d/\delta)}{n^2} \right). \quad (\text{F.8})$$

1004 **F.4. Final Bound**

1005 Combining Eq.(F.5) and Eq.(F.8), we obtain that

$$1006 \quad \mathcal{E}(\widehat{\mathbf{w}}_t) \leq \frac{1}{\eta t \beta^2} + \eta t \log t \cdot \left(\frac{\sigma^2 \text{Tr}(\mathbf{R} \boldsymbol{\Sigma} \mathbf{R}) \log(d/\delta)}{n} + \frac{\sigma^2 s \text{Tr}(\boldsymbol{\Sigma}) \log^2(d/\delta)}{n^2} \right)$$

$$1007 \quad \lesssim \frac{\log t}{\beta} \sqrt{\frac{\sigma^2 \text{Tr}(\mathbf{R} \boldsymbol{\Sigma} \mathbf{R}) \log(d/\delta)}{n} + \frac{\sigma^2 s \text{Tr}(\boldsymbol{\Sigma}) \log^2(d/\delta)}{n^2}},$$

1008 when $\eta t \simeq \frac{1}{\beta} \cdot \left(\frac{\sigma^2 \text{Tr}(\mathbf{R} \boldsymbol{\Sigma} \mathbf{R}) \log(d/\delta)}{n} + \frac{\sigma^2 s \text{Tr}(\boldsymbol{\Sigma}) \log^2(d/\delta)}{n^2} \right)^{-1/2}$.

1009 **F.5. Proof for Appendix F**

1010 *Proof of Lemma F.1.* Since $y_i = \sum_{j=1}^d w_j^* x_{ij} + \epsilon_i$, then we have

$$1011 \quad \widehat{r}_i = \frac{1}{n} \sum_{j=1}^n x_{ji} y_j = \frac{1}{n} \sum_{j=1}^n x_{ji} \cdot \left(\sum_{k=1}^d w_k^* x_{jk} + \epsilon_j \right) = \sum_{k=1}^d \frac{w_k^*}{n} \sum_{j=1}^n x_{jk} x_{ji} + \frac{1}{n} \sum_{j=1}^n x_{ji} \epsilon_j. \quad (\text{F.9})$$

1012 Since $x_{ji} \sim \text{N}(0, \Sigma_{ii})$ for any i, j , by Lemma 2.7.7 in Vershynin (2020), there exists an absolute constant C such that $x_{jk} x_{ji}$ is a sub-exponential random variable with

$$1013 \quad \|x_{jk} x_{ji}\|_{\Psi_1} \leq C \sqrt{\Sigma_{kk} \Sigma_{ii}} \leq K,$$

1014 where $\|\cdot\|_{\Psi_1}$ denotes the sub-exponential norm and the last inequality comes from the definition of K . By applying Bernstein's inequality (Theorem 2.8.1) in Vershynin (2020), we have

$$1015 \quad \left| \frac{1}{n} \sum_{j=1}^n x_{jk} x_{ji} - \mathbb{E}[x_{1k} x_{1i}] \right| = \left| \frac{1}{n} \sum_{j=1}^n x_{jk} x_{ji} - \Sigma_{ki} \right|$$

$$1016 \quad \leq K \cdot \max \left\{ \sqrt{\frac{\log(d/\delta)}{n}}, \frac{\log(d/\delta)}{n} \right\}$$

$$1017 \quad = K \cdot \sqrt{\frac{\log(d/\delta)}{n}}, \quad (\text{F.10})$$

1045 where the last equality due to $n \geq \mathcal{O}(\log(d/\delta))$. We also note that $x_{ji}\epsilon_j$ is a sub-exponential random variable with
 1046 $\|x_{ji}\epsilon_j\|_{\Psi_1} \leq K$. Hence, we also have

$$1047 \left| \frac{1}{n} \sum_{j=1} x_{ji}\epsilon_j \right| \lesssim K \cdot \sqrt{\frac{\log(d/\delta)}{n}}. \quad (\text{F.11})$$

1051 Combining Eq.(F.9), Eq.(F.10) and Eq.(F.11), we have

$$1052 |\hat{r}_i - r_i| \lesssim K \cdot \sqrt{\frac{\log(d/\delta)}{n}} \sum_{k=1}^d |w_k^*| + K \cdot \sqrt{\frac{\log(d/\delta)}{n}} = (\|w^*\|_1 + 1)K \cdot \sqrt{\frac{\log(d/\delta)}{n}}.$$

1056 By definition of $\hat{\mathbf{R}}$ and \mathbf{R} , we obtain

$$1057 \|\hat{\mathbf{R}} - \mathbf{R}\|_2 = \max_i |\hat{r}_i - r_i| \leq K(\|w^*\|_1 + 1) \cdot \sqrt{\frac{\log(d/\delta)}{n}} \\ 1058 \leq K \left(\sqrt{s\|w^*\|_2^2} + 1 \right) \cdot \sqrt{\frac{\log(d/\delta)}{n}} \lesssim K \cdot \sqrt{\frac{s \log(d/\delta)}{n}},$$

1064 which completes the proof. \square

1066 *Proof of Lemma F.2.* By Lemma F.1, for any $j \in \mathcal{S}$, with probability at least $1 - \delta$, we have

$$1067 |r_i - \hat{r}_j| \lesssim \sqrt{\frac{s \log(d/\delta)}{n}} \lesssim \beta/2 \leq |r_j|/2, \quad (\text{F.12})$$

1070 where the last inequality is due to the definition of β . \square

1072 *Proof of Lemma F.4.* We can decompose $\|\hat{\mathbf{R}}\hat{\Sigma}\hat{\mathbf{R}} - \mathbf{R}\Sigma\mathbf{R}\|_2$ as follows:

$$1073 \|\hat{\mathbf{R}}\hat{\Sigma}\hat{\mathbf{R}} - \mathbf{R}\Sigma\mathbf{R}\|_2 = \|\hat{\mathbf{R}}\hat{\Sigma}\hat{\mathbf{R}} - \mathbf{R}\hat{\Sigma}\hat{\mathbf{R}} + \mathbf{R}\hat{\Sigma}\hat{\mathbf{R}} - \mathbf{R}\Sigma\hat{\mathbf{R}} + \mathbf{R}\Sigma\hat{\mathbf{R}} - \mathbf{R}\Sigma\mathbf{R}\|_2 \\ 1074 \leq \underbrace{\|\hat{\mathbf{R}}\hat{\Sigma}\hat{\mathbf{R}} - \mathbf{R}\hat{\Sigma}\hat{\mathbf{R}}\|_2}_{\text{I}} + \underbrace{\|\mathbf{R}\hat{\Sigma}\hat{\mathbf{R}} - \mathbf{R}\Sigma\hat{\mathbf{R}}\|_2}_{\text{II}} + \underbrace{\|\mathbf{R}\Sigma\hat{\mathbf{R}} - \mathbf{R}\Sigma\mathbf{R}\|_2}_{\text{III}}. \quad (\text{F.13})$$

1078 Next, we proof the bound for I, II and III separately.

1080 For term I,

$$1081 \text{I} = \|\hat{\mathbf{R}}\hat{\Sigma}\hat{\mathbf{R}} - \mathbf{R}\hat{\Sigma}\hat{\mathbf{R}}\|_2 = \|(\hat{\mathbf{R}} - \mathbf{R})\hat{\Sigma}\hat{\mathbf{R}}\|_2 \\ 1082 \leq \|\hat{\mathbf{R}} - \mathbf{R}\|_2 \cdot \|\hat{\Sigma}\|_2 \cdot \|\hat{\mathbf{R}}\|_2 \\ 1083 \leq \|\hat{\mathbf{R}} - \mathbf{R}\|_2 \cdot \left(\|\Sigma\|_2 + \|\hat{\Sigma} - \Sigma\|_2 \right) \cdot \left(\|\mathbf{R}\|_2 + \|\mathbf{R} - \hat{\mathbf{R}}\|_2 \right), \quad (\text{F.14})$$

1087 where the last line is due to triangle inequality. By Lemma F.3, with probability at least $1 - \delta/3$, we have

$$1088 \|\hat{\Sigma} - \Sigma\|_2 \lesssim \|\Sigma\|_2 \cdot \max \left\{ \sqrt{\frac{r(\Sigma)}{n}}, \frac{r(\Sigma)}{n}, \sqrt{\frac{\log(1/\delta)}{n}}, \frac{\log(1/\delta)}{n} \right\} \\ 1089 \lesssim \|\Sigma\|_2 \cdot \max \left\{ \sqrt{\frac{r(\Sigma) + \log(1/\delta)}{n}}, \frac{r(\Sigma) + \log(1/\delta)}{n} \right\}. \quad (\text{F.15})$$

1095 By Lemma F.1, we obtain that

$$1096 \|\hat{\mathbf{R}} - \mathbf{R}\|_2 \leq K \cdot \sqrt{\frac{s \log(d/\delta)}{n}} \lesssim 1 \quad (\text{F.16})$$

1100 holds with probability at least $1 - \delta/3$, where the last inequality is valid since $n \gtrsim K^2 s \|\mathbf{R}\|_2^2 \log(d/\delta)$. Combing Eq.(F.14),
 1101 Eq.(F.15) and Eq.(F.16), we have

$$\begin{aligned}
 1102 & \\
 1103 & \\
 1104 & \\
 1105 & \text{I} \lesssim K \|\boldsymbol{\Sigma}\|_2 \sqrt{\frac{s \log(d/\delta)}{n}} \cdot \left(1 + \max \left\{ \sqrt{\frac{r(\boldsymbol{\Sigma}) + \log(1/\delta)}{n}}, \frac{r(\boldsymbol{\Sigma}) + \log(1/\delta)}{n} \right\} \right) \\
 1106 & \\
 1107 & \\
 1108 & \leq K \|\boldsymbol{\Sigma}\|_2 \sqrt{\frac{s \log(d/\delta)}{n}} \cdot \left(1 + \sqrt{\frac{r(\boldsymbol{\Sigma}) + \log(1/\delta)}{n}} + \frac{r(\boldsymbol{\Sigma}) + \log(1/\delta)}{n} \right). \tag{F.17} \\
 1109 & \\
 1110 & \\
 1111 & \\
 1112 &
 \end{aligned}$$

1113 For term II, we can decompose II as follows:

$$\begin{aligned}
 1114 & \\
 1115 & \\
 1116 & \|\mathbf{R}(\widehat{\boldsymbol{\Sigma}} - \boldsymbol{\Sigma})\widehat{\mathbf{R}}\|_2 \leq \underbrace{\|\mathbf{R}(\widehat{\boldsymbol{\Sigma}} - \boldsymbol{\Sigma})\mathbf{R}\|_2}_{\text{II.a}} + \underbrace{\|\mathbf{R}(\widehat{\boldsymbol{\Sigma}} - \boldsymbol{\Sigma})(\widehat{\mathbf{R}} - \mathbf{R})\|_2}_{\text{II.b}}. \\
 1117 & \\
 1118 & \\
 1119 & \\
 1120 &
 \end{aligned}$$

1121 For term II.a, by using Lemma F.3, we have with probability at least $1 - \delta/3$,

$$\begin{aligned}
 1122 & \\
 1123 & \\
 1124 & \\
 1125 & \text{II.a} \lesssim \|\mathbf{R}\boldsymbol{\Sigma}\mathbf{R}\|_2 \cdot \max \left\{ \sqrt{\frac{r(\mathbf{R}\boldsymbol{\Sigma}\mathbf{R})}{n}}, \frac{r(\mathbf{R}\boldsymbol{\Sigma}\mathbf{R})}{n}, \sqrt{\frac{\log(1/\delta)}{n}}, \frac{\log(1/\delta)}{n} \right\} \\
 1126 & \\
 1127 & \\
 1128 & \lesssim \|\mathbf{R}\boldsymbol{\Sigma}\mathbf{R}\|_2 \cdot \max \left\{ \sqrt{\frac{r(\mathbf{R}\boldsymbol{\Sigma}\mathbf{R}) + \log(1/\delta)}{n}}, \frac{r(\mathbf{R}\boldsymbol{\Sigma}\mathbf{R}) + \log(1/\delta)}{n} \right\} \\
 1129 & \\
 1130 & \\
 1131 & \leq \|\mathbf{R}\boldsymbol{\Sigma}\mathbf{R}\|_2 \cdot \left(\sqrt{\frac{r(\mathbf{R}\boldsymbol{\Sigma}\mathbf{R}) + \log(1/\delta)}{n}} + \frac{r(\mathbf{R}\boldsymbol{\Sigma}\mathbf{R}) + \log(1/\delta)}{n} \right) \tag{F.18} \\
 1132 & \\
 1133 & \\
 1134 & \\
 1135 &
 \end{aligned}$$

1136 Similar to the proof for bounding I, we can obtain that

$$\begin{aligned}
 1137 & \\
 1138 & \\
 1139 & \\
 1140 & \text{II.b} \lesssim K \|\boldsymbol{\Sigma}\|_2 \sqrt{\frac{s \log(d/\delta)}{n}} \cdot \left(1 + \sqrt{\frac{r(\boldsymbol{\Sigma}) + \log(1/\delta)}{n}} + \frac{r(\boldsymbol{\Sigma}) + \log(1/\delta)}{n} \right). \tag{F.19} \\
 1141 & \\
 1142 & \\
 1143 &
 \end{aligned}$$

1144 For term III, we have

$$\begin{aligned}
 1145 & \\
 1146 & \\
 1147 & \\
 1148 & \text{III} = \|\mathbf{R}\boldsymbol{\Sigma}(\widehat{\mathbf{R}} - \mathbf{R})\|_2 \leq \|\mathbf{R}\|_2 \|\boldsymbol{\Sigma}\|_2 K (\|\mathbf{w}^*\|_1 + 1) \cdot \sqrt{\frac{s \log(d/\delta)}{n}}, \tag{F.20} \\
 1149 & \\
 1150 & \\
 1151 &
 \end{aligned}$$

1152 where the last inequality is by Eq.(F.16).

1153 Combining Eq.(F.17), Eq.(F.18), Eq.(F.19) and Eq.(F.20) and taking the union bound, we obtain that with probability at
 1154

1155 least $1 - \delta$,

$$\begin{aligned}
 &1156 \|\widehat{\mathbf{R}}\widehat{\Sigma}\widehat{\mathbf{R}} - \mathbf{R}\Sigma\mathbf{R}\|_2 \leq \text{I} + \text{II} + \text{III} \\
 &1157 \lesssim K\|\Sigma\|_2(\|\mathbf{w}^*\|_1 + 1)\sqrt{\frac{\log(d/\delta)}{n}} \cdot \left(1 + \sqrt{\frac{r(\Sigma) + \log(1/\delta)}{n}} + \frac{r(\Sigma) + \log(1/\delta)}{n}\right) \\
 &1158 + \|\mathbf{R}\Sigma\mathbf{R}\|_2 \cdot \left(\sqrt{\frac{r(\mathbf{R}\Sigma\mathbf{R}) + \log(1/\delta)}{n}} + \frac{r(\mathbf{R}\Sigma\mathbf{R}) + \log(1/\delta)}{n}\right) \\
 &1159 + \|\mathbf{R}\|_2\|\Sigma\|_2K(\|\mathbf{w}^*\|_1 + 1) \cdot \sqrt{\frac{\log(d/\delta)}{n}} \\
 &1160 \leq (K\|\Sigma\|_2(\|\mathbf{w}^*\|_1 + 1) + \|\mathbf{R}\Sigma\mathbf{R}\|_2 + \|\mathbf{R}\|_2\|\Sigma\|_2K(\|\mathbf{w}^*\|_1 + 1)) \\
 &1161 \cdot \left(\sqrt{\frac{\log(d/\delta)}{n}} \cdot \left(2 + \sqrt{\frac{r(\Sigma) + \log(1/\delta)}{n}} + \frac{r(\Sigma) + \log(1/\delta)}{n}\right)\right) \\
 &1162 + \sqrt{\frac{r(\mathbf{R}\Sigma\mathbf{R}) + \log(1/\delta)}{n}} + \frac{r(\mathbf{R}\Sigma\mathbf{R}) + \log(1/\delta)}{n} \\
 &1163 \lesssim \widetilde{C}_{\text{cov}} \cdot \left(\sqrt{\frac{r(\mathbf{R}\Sigma\mathbf{R}) + \log(1/\delta)}{n}} + \frac{\sqrt{r(\Sigma)\log(d/\delta)} + r(\mathbf{R}\Sigma\mathbf{R}) + \log(d/\delta)}{n}\right) \\
 &1164 + \frac{r(\Sigma)\sqrt{\log(d/\delta)} + \log^{3/2}(d/\delta)}{n^{3/2}} \\
 &1165 \lesssim \widetilde{C}_{\text{cov}} \cdot \text{poly}(\log(d/\delta)) \cdot \left(\sqrt{\frac{r(\mathbf{R}\Sigma\mathbf{R})}{n}} + \frac{\sqrt{r(\Sigma)} + r(\mathbf{R}\Sigma\mathbf{R})}{n} + \frac{r(\Sigma)}{n^{3/2}}\right), \\
 &1166 \\
 &1167 \\
 &1168 \\
 &1169 \\
 &1170 \\
 &1171 \\
 &1172 \\
 &1173 \\
 &1174 \\
 &1175 \\
 &1176 \\
 &1177 \\
 &1178 \\
 &1179 \\
 &1180 \\
 &1181
 \end{aligned}$$

1182 where the second last inequality is by $aa' + bb' + cc' \leq (a + b + c)(a' + b' + c')$ for $a, a', b, b', c, c' \geq 0$. Here $\widetilde{C}_{\text{cov}} =$
 1183 $K\|\Sigma\|_2(\|\mathbf{w}^*\|_1 + 1) + \|\mathbf{R}\Sigma\mathbf{R}\|_2 + \|\mathbf{R}\|_2\|\Sigma\|_2K(\|\mathbf{w}^*\|_1 + 1) \lesssim \sqrt{s}$. \square

1185 *Proof of Lemma F.5.* By the triangle inequality, we have

$$\begin{aligned}
 &1186 \left\|\widehat{\mathbf{R}}(\Sigma - \widehat{\Sigma})\widehat{\mathbf{R}}\right\|_2 \\
 &1187 = \left\|\mathbf{R}(\Sigma - \widehat{\Sigma})\mathbf{R} + \mathbf{R}(\Sigma - \widehat{\Sigma})(\widehat{\mathbf{R}} - \mathbf{R}) + (\widehat{\mathbf{R}} - \mathbf{R})(\Sigma - \widehat{\Sigma})\mathbf{R} + (\widehat{\mathbf{R}} - \mathbf{R})(\Sigma - \widehat{\Sigma})(\widehat{\mathbf{R}} - \mathbf{R})\right\|_2 \\
 &1188 \leq \left\|\mathbf{R}(\Sigma - \widehat{\Sigma})\mathbf{R}\right\|_2 + \left\|\mathbf{R}(\Sigma - \widehat{\Sigma})(\widehat{\mathbf{R}} - \mathbf{R})\right\|_2 + \left\|(\widehat{\mathbf{R}} - \mathbf{R})(\Sigma - \widehat{\Sigma})\mathbf{R}\right\|_2 + \left\|(\widehat{\mathbf{R}} - \mathbf{R})(\Sigma - \widehat{\Sigma})(\widehat{\mathbf{R}} - \mathbf{R})\right\|_2. \\
 &1189 \\
 &1190 \\
 &1191 \\
 &1192
 \end{aligned}$$

1193 Following the proof of Lemma F.4, we can prove that with probability at least $1 - \delta$,

$$\left\|\widehat{\mathbf{R}}(\Sigma - \widehat{\Sigma})\widehat{\mathbf{R}}\right\|_2 \lesssim \widetilde{\alpha}(n, \delta) \leq 1/t, \tag{F.21}$$

1196 where the last inequality is by \mathcal{E}_2 . By Eq.(F.21), we have

$$\widehat{\mathbf{R}}(\Sigma - \widehat{\Sigma})\widehat{\mathbf{R}} \preceq 1/t \cdot \mathbf{I}.$$

1199 Hence, we obtain that

$$\begin{aligned}
 &1200 \mathbf{I} \lesssim \mathbf{w}^{*\top} \overline{\mathbf{R}}(\mathbf{I} - \eta\widehat{\Sigma})^t \cdot 1/t \cdot \mathbf{I} \cdot (\mathbf{I} - \eta\widehat{\Sigma})^t \overline{\mathbf{R}}\mathbf{w}^* \\
 &1201 = \frac{1}{t} \mathbf{w}^{*\top} \overline{\mathbf{R}}(\mathbf{I} - \eta\widehat{\Sigma})^{2t} \overline{\mathbf{R}}\mathbf{w}^* \\
 &1202 \leq \frac{1}{t} \mathbf{w}^{*\top} \overline{\mathbf{R}}\overline{\mathbf{R}}\mathbf{w}^* \quad (\text{by } (\mathbf{I} - \eta\widehat{\Sigma})^{2t} \preceq \mathbf{I}) \\
 &1203 \leq \frac{1}{t} \|\mathbf{w}^*\|_2^2, \tag{F.22} \\
 &1204 \\
 &1205 \\
 &1206 \\
 &1207 \\
 &1208 \\
 &1209
 \end{aligned}$$

1210 where the last line by $\overline{\mathbf{R}} \preceq \frac{2}{\beta} \cdot \mathbf{I}$. For the term II, we have

$$\begin{aligned}
 1211 & \\
 1212 & \text{II} = \mathbf{w}^* \top \overline{\mathbf{R}} \left(\mathbf{I} - \eta \widehat{\Sigma} \right)^t \widehat{\mathbf{R}} \widehat{\Sigma} \widehat{\mathbf{R}} \left(\mathbf{I} - \eta \widehat{\Sigma} \right)^t \overline{\mathbf{R}} \mathbf{w}^* \\
 1213 & \lesssim \frac{1}{\eta t} \mathbf{w}^* \top \overline{\mathbf{R}} \overline{\mathbf{R}} \mathbf{w}^* \\
 1214 & \frac{1}{\eta t \beta^2} \|\mathbf{w}^*\|_2^2 \leq \frac{1}{\eta t \beta^2}, \tag{F.23} \\
 1215 & \\
 1216 & \\
 1217 & \\
 1218 &
 \end{aligned}$$

1219 where the second last line is by the fact that $x(1-x)^k \leq 1/(k+1)$ for all $x \in [0, 1]$ and all $k > 0$. \square

1221 *Proof of Lemma F.6.* Similar to the proof of Lemma F.5, with probability at least $1 - \delta$, we have $\widehat{\mathbf{R}} \left(\Sigma - \widehat{\Sigma} \right) \widehat{\mathbf{R}} \preceq \frac{1}{t} \cdot \mathbf{I}$.

1222 Then we have

$$\begin{aligned}
 1223 & \\
 1224 & \text{I} = \frac{\eta^2}{n^2} \epsilon^\top \mathbf{X} \widehat{\mathbf{R}} \sum_{i=1}^t \left(\mathbf{I} - \eta \widehat{\Sigma} \right)^{i-1} \widehat{\mathbf{R}} \left(\Sigma - \widehat{\Sigma} \right) \widehat{\mathbf{R}} \sum_{i=1}^t \left(\mathbf{I} - \eta \widehat{\Sigma} \right)^{i-1} \widehat{\mathbf{R}} \mathbf{X}^\top \epsilon \\
 1225 & \lesssim \frac{\eta^2}{tn^2} \epsilon^\top \mathbf{X} \widehat{\mathbf{R}} \sum_{i=1}^t \left(\mathbf{I} - \eta \widehat{\Sigma} \right)^{i-1} \sum_{i=1}^t \left(\mathbf{I} - \eta \widehat{\Sigma} \right)^{i-1} \widehat{\mathbf{R}} \mathbf{X}^\top \epsilon \\
 1226 & \leq \frac{\eta^2 t}{n^2} \epsilon^\top \mathbf{X} \widehat{\mathbf{R}} \widehat{\mathbf{R}} \mathbf{X}^\top \epsilon \\
 1227 & = \frac{\eta^2 t}{n^2} \cdot \left\| \widehat{\mathbf{R}} \mathbf{X}^\top \epsilon \right\|_2^2, \\
 1228 & \\
 1229 & \\
 1230 & \\
 1231 & \\
 1232 & \\
 1233 &
 \end{aligned}$$

1234 where the second last line is by $\sum_{i=1}^t \left(\mathbf{I} - \eta \widehat{\Sigma} \right)^{i-1} \preceq t \cdot \mathbf{I}$. By the fact that $x(1-x)^k \leq 1/(k+1)$ for all $x \in [0, 1]$ and all $k > 0$, we have

$$\begin{aligned}
 1235 & \\
 1236 & \text{II} = \frac{\eta^2}{n^2} \epsilon^\top \mathbf{X} \widehat{\mathbf{R}} \sum_{i=1}^t \left(\mathbf{I} - \eta \widehat{\Sigma} \right)^{i-1} \widehat{\mathbf{R}} \widehat{\Sigma} \widehat{\mathbf{R}} \sum_{i=1}^t \left(\mathbf{I} - \eta \widehat{\Sigma} \right)^{i-1} \widehat{\mathbf{R}} \mathbf{X}^\top \epsilon \\
 1237 & = \frac{\eta}{n^2} \epsilon^\top \mathbf{X} \widehat{\mathbf{R}} \left(\sum_{i,j=1}^t \left(\mathbf{I} - \eta \widehat{\Sigma} \right)^{i+j-2} \eta \widehat{\mathbf{R}} \widehat{\Sigma} \right) \widehat{\mathbf{R}} \mathbf{X}^\top \epsilon \\
 1238 & \leq \frac{\eta}{n^2} \cdot \left(\sum_{i,j=1}^t \frac{1}{i+j-1} \right) \left\| \widehat{\mathbf{R}} \mathbf{X}^\top \epsilon \right\|_2^2 \\
 1239 & \leq \frac{\eta t}{n^2} \cdot \left(\sum_{i=1}^t \frac{1}{i} \right) \left\| \widehat{\mathbf{R}} \mathbf{X}^\top \epsilon \right\|_2^2 \\
 1240 & \lesssim \frac{\eta t \log t}{n^2} \cdot \left\| \widehat{\mathbf{R}} \mathbf{X}^\top \epsilon \right\|_2^2, \\
 1241 & \\
 1242 & \\
 1243 & \\
 1244 & \\
 1245 & \\
 1246 & \\
 1247 & \\
 1248 & \\
 1249 & \\
 1250 & \\
 1251 &
 \end{aligned}$$

1252 where the last inequality is by the fact that $\sum_{i=1}^t \frac{1}{i} \lesssim \log t$. \square

1253 *Proof of Lemma F.7.* First, we can decompose $\left\| \frac{1}{n} \cdot \widehat{\mathbf{R}} \mathbf{X}^\top \epsilon \right\|_2^2$ by

$$\left\| \frac{1}{n} \cdot \widehat{\mathbf{R}} \mathbf{X}^\top \epsilon \right\|_2^2 \lesssim \left\| \frac{1}{n} \cdot \mathbf{R} \mathbf{X}^\top \epsilon \right\|_2^2 + \left\| \frac{1}{n} \cdot \left(\widehat{\mathbf{R}} - \mathbf{R} \right) \mathbf{X}^\top \epsilon \right\|_2^2.$$

1257 Let $\mathbf{z}_i = \mathbf{R} \mathbf{x}_i$, then $\mathbf{z}_i \sim \mathbf{N}(\mathbf{G})$, where $\mathbf{G} := \mathbf{R} \Sigma \mathbf{R}$. For any i, j , by Lemma 2.7.7 in Vershynin (2020), there exists an absolute constant C such that $\epsilon_j z_{ji}$ is a sub-exponential random variable with

$$\|\epsilon_j z_{ji}\|_{\Psi_1} \leq C \sigma \sqrt{G_{ii}}.$$

1264

1265 By applying Bernstein's inequality [Vershynin \(2020, Theorem 2.8.1\)](#), for any $1 \leq i \leq d$, we have that

$$\begin{aligned}
 1266 & \left| \frac{1}{n} \sum_{j=1}^n \epsilon_j z_{ji} - \mathbb{E}[\epsilon_1 z_{1i}] \right| = \left| \frac{1}{n} \sum_{j=1}^n \epsilon_j z_{ji} \right| \\
 1267 & \\
 1268 & \\
 1269 & \\
 1270 & \lesssim \sigma \sqrt{G_{ii}} \cdot \max \left\{ \sqrt{\frac{\log(d/\delta)}{n}}, \frac{\log(d/\delta)}{n} \right\} = \sigma \sqrt{G_{ii}} \cdot \sqrt{\frac{\log(d/\delta)}{n}} \\
 1271 & \\
 1272 &
 \end{aligned} \tag{F.24}$$

1273 hold with probability $1 - \frac{\delta}{3d}$, where the last inequality is due to $n \geq \mathcal{O}(\log(d/\delta))$. By taking the union bound, we obtain
1274 that

$$\left| \frac{1}{n} \sum_{j=1}^n \epsilon_j z_{ji} \right| \lesssim \sigma \sqrt{G_{ii}} \cdot \sqrt{\frac{\log(d/\delta)}{n}}$$

1278 holds for any i , with probability $1 - \frac{\delta}{3}$. Then we have

$$\text{I} = \sum_{i=1}^d \left(\frac{1}{n} \sum_{j=1}^n \epsilon_j z_{ji} \right)^2 \lesssim \sum_{i=1}^d \sigma^2 G_{ii} \cdot \frac{\log(d/\delta)}{n} = \frac{\sigma^2 \text{Tr}(\mathbf{R}\Sigma\mathbf{R}) \log(d/\delta)}{n}.$$

1284 In the same way, we can prove that with probability at least $1 - \delta/3$,

$$\left\| \frac{1}{n} \mathbf{X}^\top \epsilon \right\|_2^2 \lesssim \frac{\sigma^2 \text{Tr}(\Sigma) \log(d/\delta)}{n}. \tag{F.25}$$

1288 By applying [Lemma F.1](#), with probability at least $1 - \delta/3$, we have

$$\left\| \widehat{\mathbf{R}} - \mathbf{R} \right\|_2^2 \lesssim \frac{s \log(d/\delta)}{n}. \tag{F.26}$$

1292 By [Eq.\(F.25\)](#) and [Eq.\(F.26\)](#), with probability $1 - 2\delta/3$, we have

$$\left\| \frac{1}{n} \cdot (\widehat{\mathbf{R}} - \mathbf{R}) \mathbf{X}^\top \epsilon \right\|_2^2 \leq \left\| \widehat{\mathbf{R}} - \mathbf{R} \right\|_2^2 \left\| \frac{1}{n} \mathbf{X}^\top \epsilon \right\|_2^2 \lesssim \frac{\sigma^2 s \text{Tr}(\Sigma) \log^2(d/\delta)}{n^2}.$$

1296 By taking the union bound, we derive the desired result. \square

1298 G. Proof for [Theorem E.2](#)

1300 To simplify the notations, we use \mathbf{w}_t to denote \mathbf{w}_{gd}^t .

1301 **Lemma G.1.** *with probability at least $1 - \delta$, we have*

$$\left\| \widehat{\Sigma} - \Sigma \right\| \lesssim \alpha(n, \delta), \tag{G.1}$$

1305 where $\alpha(n, \delta) = \sqrt{\frac{\text{Tr}(\Sigma) + \log(1/\delta)}{n}} + \frac{\text{Tr}(\Sigma) + \log(1/\delta)}{n}$. As a result, when $n \gtrsim t^2(\text{Tr}(\Sigma) + \log(1/\delta))$, with probability at
1306 least $1 - \delta$,

$$\left\| \widehat{\Sigma} - \Sigma \right\| \lesssim 1/t.$$

1310 *Proof of [Lemma G.1](#).* By [Lemma F.3](#), we have

$$\begin{aligned}
 1311 & \left\| \widehat{\Sigma} - \Sigma \right\|_2 \leq c \left\| \Sigma \right\|_2 \cdot \max \left\{ \sqrt{\frac{r(\Sigma)}{n}}, \frac{r(\Sigma)}{n}, \sqrt{\frac{\log(1/\delta)}{n}}, \frac{\log(1/\delta)}{n} \right\} \\
 1312 & \\
 1313 & \\
 1314 & \lesssim \max \left\{ \sqrt{\frac{r(\Sigma) + \log(1/\delta)}{n}}, \frac{r(\Sigma) + \log(1/\delta)}{n} \right\} \\
 1315 & \\
 1316 & \\
 1317 & \leq \sqrt{\frac{r(\Sigma) + \log(1/\delta)}{n}} + \frac{r(\Sigma) + \log(1/\delta)}{n} \\
 1318 & \\
 1319 &
 \end{aligned} \tag{G.2}$$

1320 holds with probability at least $1 - \delta$, where the last line is by the inequality that $\max\{a, b\} \leq a + b$ for all $a, b \geq 0$. \square

1321

1322 We define the event \mathcal{E} as follows:

1323

1324

$$\mathcal{E} := \left\{ \|\mathbf{R}\Sigma\mathbf{R}\|_2 \lesssim \alpha(n, \delta) \leq 1/t \right\}.$$

1325

1326 By Lemma G.1, $\mathbb{P}(\mathcal{E}) \geq 1 - \delta$. Hereafter, we condition on \mathcal{E} .

1327

1328 **Bias-variance Decomposition** Similar to Eq.(F.1), we have

1329

1330

$$\mathbf{w}_t = \left(\mathbf{I} - \left(\mathbf{I} - \eta \widehat{\Sigma} \right)^t \right) \mathbf{w}^* + \frac{1}{n} \sum_{i=1}^t \left(\mathbf{I} - \eta \widehat{\Sigma} \right)^{i-1} \mathbf{X}^\top \epsilon. \quad (\text{G.3})$$

1331

1332 In the same way, we can decompose the risk $\mathcal{E}(\mathbf{w}_t)$ by

1333

1334

1335

1336

$$\mathcal{E}(\mathbf{w}_t) = \underbrace{\left\| \Sigma^{1/2} \left(\mathbf{I} - \eta \widehat{\Sigma} \right)^t \mathbf{w}^* \right\|_2^2}_{\text{Bias}} + \eta^2 \underbrace{\left\| \Sigma^{1/2} \left(\frac{1}{n} \sum_{i=1}^t \left(\mathbf{I} - \eta \widehat{\Sigma} \right)^{i-1} \mathbf{X}^\top \epsilon \right) \right\|_2^2}_{\text{Variance}}. \quad (\text{G.4})$$

1337

1338

1339

Bounding the Bias

1340

1341

1342

1343

1344

$$\begin{aligned} \text{Bias} &= \mathbf{w}^{*\top} \left(\mathbf{I} - \eta \widehat{\Sigma} \right)^t \Sigma \left(\mathbf{I} - \eta \widehat{\Sigma} \right)^t \mathbf{w}^* \\ &= \underbrace{\mathbf{w}^{*\top} \left(\mathbf{I} - \eta \widehat{\Sigma} \right)^t \left(\Sigma - \widehat{\Sigma} \right) \left(\mathbf{I} - \eta \widehat{\Sigma} \right)^t \mathbf{w}^*}_{\text{I}} + \underbrace{\mathbf{w}^{*\top} \left(\mathbf{I} - \eta \widehat{\Sigma} \right)^t \widehat{\Sigma} \left(\mathbf{I} - \eta \widehat{\Sigma} \right)^t \mathbf{w}^*}_{\text{II}}. \end{aligned}$$

1345

1346 Similar to the proof of Lemma F.5, we have the following lemma.

1347

Lemma G.2. *On \mathcal{E} , we have*

1348

1349

$$\text{I} \lesssim \frac{1}{t}$$

1350

1351 *and*

1352

1353

$$\text{II} \lesssim \frac{1}{\eta t}$$

1354

1355 *hold with probability at least $1 - \delta$.*

1356

1357

As a result, the bound of the bias term is given by

1358

1359

$$\text{Bias} \leq \frac{1}{\eta t} + \frac{1}{t} \lesssim \frac{1}{\eta t}. \quad (\text{G.5})$$

1360

1361 **Bounding the Variance** By using the same way of the proof for bounding the variance term of Theorem E.1, we have the following lemma.

1362

1363

Lemma G.3. *On \mathcal{E} , with probability at least $1 - \delta$, we have that*

1364

1365

1366

1367

$$\text{Variance} \lesssim \eta t \log t \cdot \left\| \frac{1}{n} \cdot \mathbf{X}^\top \epsilon \right\|_2^2 \lesssim \eta t \log t \cdot \frac{\sigma^2 \text{Tr}(\Sigma) \log(d/\delta)}{n}. \quad (\text{G.6})$$

1368

1369

Combining Eq.(G.5) and Eq.(G.6), we obtain that

1370

1371

1372

$$\mathcal{E}(\mathbf{w}_t) \lesssim \frac{1}{\eta t} + \eta t \log t \cdot \frac{\sigma^2 \text{Tr}(\Sigma) \log(d/\delta)}{n} \lesssim \log t \cdot \sqrt{\frac{\sigma^2 \text{Tr}(\Sigma) \log(d/\delta)}{n}},$$

1373

1374

when $\eta t \simeq \left(\frac{\sigma^2 \text{Tr}(\Sigma) \log(d/\delta)}{n} \right)^{-1/2}$

1375 H. Proof for Theorem 5.1

1376 To simplify the notation, we use $\widehat{\mathbf{w}}_t$ to denote $\widetilde{\mathbf{w}}_{\text{gd}}^t$ and \mathbf{w}_t to denote \mathbf{w}_{gd}^t .

1378 H.1. Proof for the upper bound of the excess risk

1379 When $\Sigma = \mathbf{I}$, by Eq.(F.2), we have

$$1380 \mathcal{E}(\widehat{\mathbf{w}}_t) = \underbrace{\left\| \widehat{\mathbf{R}}(\mathbf{I} - \eta \widehat{\Sigma})^t \overline{\mathbf{R}} \mathbf{w}^* \right\|_2^2}_{\text{Bias}} + \eta^2 \underbrace{\left\| \widehat{\mathbf{R}} \left(\frac{1}{n} \sum_{i=1}^t (\mathbf{I} - \eta \widehat{\Sigma})^{i-1} \widetilde{\mathbf{X}}^\top \epsilon \right) \right\|_2^2}_{\text{Variance}}.$$

1386 Following the proof of Theorem E.1, it holds that

$$1387 \text{Variance} \lesssim \eta t \log t \cdot \frac{\sigma^2 \log(d/\delta)}{n} + \frac{\sigma^2 s d \log^2(d/\delta)}{n^2}$$

1388 with probability at least $1 - \delta$, when $n \gtrsim t^2 s d^{2/3}$

1389 Similar to the proof of Lemma F.2, we can prove that

$$1390 \widehat{r}_i \geq \frac{r_i}{2} \quad \forall i \in \mathcal{S}, \quad \widehat{r}_i \lesssim 1 \quad \forall i,$$

1391 with probability at least $1 - \delta$.

1392 When $\Sigma = \mathbf{I}$, by Lemma F.4, we have that

$$1393 \left\| \widehat{\mathbf{R}} \widehat{\Sigma} \widehat{\mathbf{R}} - \mathbf{R} \Sigma \mathbf{R} \right\|_2 \lesssim \frac{\beta^2}{t}$$

1394 holds with probability at least $1 - \delta$, when $n \gtrsim \frac{t^2 \|\mathbf{w}^*\|_1^2 d^{2/3}}{\beta^4}$. As a result, $\mathbf{R} \Sigma \mathbf{R} - \frac{\beta^2}{t} \cdot \mathbf{I} \preceq \widehat{\mathbf{R}} \widehat{\Sigma} \widehat{\mathbf{R}}$. Hereafter, we condition on the above events. For the bias term, we have

$$\begin{aligned} 1400 \left\| \widehat{\mathbf{R}}(\mathbf{I} - \eta \widehat{\Sigma})^t \overline{\mathbf{R}} \mathbf{w}^* \right\|_2^2 &\leq \left\| \widehat{\mathbf{R}} \right\|_2^2 \cdot \left\| (\mathbf{I} - \eta \widehat{\Sigma})^t \overline{\mathbf{R}} \mathbf{w}^* \right\|_2^2 \\ 1401 &\leq \mathbf{w}^{*\top} \overline{\mathbf{R}} (\mathbf{I} - \eta \widehat{\Sigma})^{2t} \overline{\mathbf{R}} \mathbf{w}^* \\ 1402 &\lesssim \mathbf{w}^{*\top} \overline{\mathbf{R}} \left(\mathbf{I} - \eta \left(\mathbf{R} \Sigma \mathbf{R} - \frac{\beta^2}{t} \cdot \mathbf{I} \right) \right)^{2t} \overline{\mathbf{R}} \mathbf{w}^* \\ 1403 &= \sum_{i \in \mathcal{S}} (w_i^* / \widehat{r}_i)^2 \cdot \left(1 - \eta \left((w_i^*)^2 - \frac{\beta^2}{t} \right) \right)^{2t} \\ 1404 &\leq s \cdot (1 - \eta \beta^2 / 2)^{2t}, \end{aligned}$$

1405 where the last line is by the definition of β . When $t \gtrsim \log\left(\frac{\sigma^2}{ns}\right) / (2 \log(1 - \eta \beta^2 / 2))$, we have

$$1406 \text{Bias} = \left\| \widehat{\mathbf{R}}(\mathbf{I} - \eta \widehat{\Sigma})^t \overline{\mathbf{R}} \mathbf{w}^* \right\|_2^2 \leq \frac{\sigma^2}{n}. \quad (\text{H.1})$$

1407 When $\eta \beta^2 / 2 \leq 1/2$, there exist a $c > 0$, such that

$$1408 \log(1 - \eta \beta^2 / 2) \geq c \eta \beta^2 / 2.$$

1409 Hence, the variance term is bounded by

$$\begin{aligned} 1410 \text{Variance} &\lesssim \eta t \log t \cdot \left(\frac{\sigma^2 \log(d/\delta)}{n} + \frac{\sigma^2 \|\mathbf{w}^*\|_1^2 d \log^2(d/\delta)}{n^2} \right) \\ 1411 &\lesssim \frac{\sigma^2 \log^2(ns/\sigma^2) \log^2(d/\delta)}{\beta^2} \cdot \left(\frac{s}{n} + \frac{ds}{n^2} \right), \end{aligned} \quad (\text{H.2})$$

where the last line is by $\|\mathbf{w}^*\|_1 \leq s \cdot \|\mathbf{w}^*\|_2^2 = s$ and $\eta t \lesssim \frac{\log(ns/\sigma^2)}{\beta^2}$. Combining Eq.(H.1) and Eq.(H.2), we have that

$$\mathcal{E}(\widehat{\mathbf{w}}_t) \lesssim \frac{\sigma^2}{n} + \frac{\sigma^2 \log^2(ns/\sigma^2) \log^2(d/\delta)}{\beta^2} \cdot \left(\frac{1}{n} + \frac{ds}{n^2} \right) \lesssim \frac{\sigma^2 \log^2(ns/\sigma^2) \log^2(d/\delta)}{\beta^2} \cdot \left(\frac{1}{n} + \frac{ds}{n^2} \right),$$

when $n \gtrsim \frac{t^2 s d^{2/3}}{\beta^4} \geq \frac{t^2 \|\mathbf{w}^*\|_1^2 d^{2/3}}{\beta^4}$ and $t \gtrsim \frac{\log(ns)}{\eta \beta^2}$. When $w_i^* \in \mathcal{U}\{-1/\sqrt{s}, 1/\sqrt{s}\}$, $\beta = 1/\sqrt{s}$. In this case, we have that

$$\mathcal{E}(\widehat{\mathbf{w}}_t) \lesssim \sigma^2 \log^2(ns/\sigma^2) \log^2(d/\delta) \cdot \left(\frac{s}{n} + \frac{ds^2}{n^2} \right),$$

when $n \gtrsim t^2 s^3 d^{2/3}$ and $t \gtrsim \frac{\log(ns)}{\eta s}$.

H.2. Lower bound for Ridge Regression

When $n \gtrsim d + \log(1/\delta)$, by Lemma F.3, we have that $\frac{1}{2} \cdot \mathbf{I} \preceq \widehat{\Sigma} \preceq 2 \cdot \mathbf{I}$. For the ridge estimator $\widehat{\mathbf{w}}_\lambda = \frac{1}{n} \cdot (\widehat{\Sigma} + \lambda \cdot \mathbf{I})^{-1} \mathbf{X}^\top \mathbf{y}$, we have

$$\begin{aligned} \mathbb{E}_{\mathbf{w}^*}[\mathcal{E}(\widehat{\mathbf{w}}_\lambda)] &= \left\| \left(\mathbf{I} - (\widehat{\Sigma} + \lambda \mathbf{I})^{-1} \widehat{\Sigma} \right) \mathbf{w}^* \right\|_2^2 + \left\| \frac{1}{n} \cdot (\widehat{\Sigma} + \lambda \cdot \mathbf{I})^{-1} \mathbf{X}^\top \epsilon \right\|_2^2 \\ &\geq \left\| \frac{1}{n} \cdot (\widehat{\Sigma} + \lambda \cdot \mathbf{I})^{-1} \mathbf{X}^\top \epsilon \right\|_2^2. \end{aligned}$$

By Lemma F.3, when $\frac{1}{2} \cdot \mathbf{I} \preceq \widehat{\Sigma} \preceq 2 \cdot \mathbf{I}$, with probability at least $1 - \delta$, we have

$$\begin{aligned} \mathbb{E}_{\mathbf{w}^*}[\mathcal{E}(\widehat{\mathbf{w}}_\lambda)] &\geq \left\| \frac{1}{n} \cdot (\widehat{\Sigma} + \lambda \cdot \mathbf{I})^{-1} \mathbf{X}^\top \epsilon \right\|_2^2 \\ &= \frac{1}{n^2} \cdot \epsilon^\top \mathbf{X} (\widehat{\Sigma} + \lambda \mathbf{I})^{-2} \mathbf{X}^\top \epsilon \\ &\geq \frac{1}{n^2 (2 + \lambda)^2} \cdot \epsilon^\top \mathbf{X} \mathbf{X}^\top \epsilon, \end{aligned}$$

where the last line is due to the fact that $\widehat{\Sigma} + \lambda \mathbf{I} \preceq (2 + \lambda) \cdot \mathbf{I}$.

Lemma H.1. Given X such that $\frac{1}{2} \mathbf{I} \preceq \widehat{\Sigma} \preceq 2 \mathbf{I}$, it holds that

$$\left\| \frac{1}{n} \mathbf{X}^\top \epsilon \right\|_2^2 \gtrsim \frac{\sigma^2 d}{n},$$

with probability at least $1 - \delta$, when $n \geq \mathcal{O}(\log(1/\delta))$.

Proof of Lemma H.1. We consider the singular value decomposition of $\frac{1}{\sqrt{n}} \mathbf{X}^\top$: $\frac{1}{\sqrt{n}} \mathbf{X}^\top = \mathbf{U} \mathbf{\Lambda} \mathbf{V}^\top$, where $\mathbf{U} \in \mathbb{R}^{d \times d}$ is an orthogonal matrix, $\mathbf{\Lambda} \in \mathbb{R}^{d \times n}$ is a rectangular diagonal matrix with non-negative real numbers on the diagonal, $\mathbf{V} \in \mathbb{R}^{n \times n}$ is an orthogonal matrix. Let $\{\sigma_1, \dots, \sigma_d\}$ be the singular values of $\frac{1}{\sqrt{n}} \mathbf{X}^\top$. Then we have

$$\begin{aligned} \left\| \frac{1}{n} \mathbf{X}^\top \epsilon \right\|_2^2 &= \left\| \frac{1}{\sqrt{n}} \mathbf{U} \mathbf{\Lambda} \mathbf{V}^\top \epsilon \right\|_2^2 = \left\| \frac{1}{\sqrt{n}} \mathbf{\Lambda} \mathbf{V}^\top \epsilon \right\|_2^2 \\ &= \left\| \frac{1}{\sqrt{n}} \mathbf{\Lambda} \tilde{\epsilon} \right\|_2^2 = \frac{1}{n} \sum_{i=1}^d \sigma_i^2 \tilde{\epsilon}_i^2, \end{aligned}$$

1485 where $\tilde{\epsilon} = \mathbf{V}^\top \epsilon \sim \mathcal{N}(\mathbf{0}, \mathbf{I})$. By [Lemma 22], we have

$$\begin{aligned}
 1486 \quad & \left\| \frac{1}{n} \mathbf{X}^\top \epsilon \right\|_2^2 - \mathbb{E} \left[\left\| \frac{1}{n} \mathbf{X}^\top \epsilon \right\|_2^2 \right] \lesssim \sigma^2 \max \left\{ \frac{\sqrt{\sum_{i=1}^d \sigma_i^4 \log(1/\delta)}}{n}, \frac{\max_i \sigma_i^2 \log(1/\delta)}{n} \right\} \\
 1487 \quad & \\
 1488 \quad & \\
 1489 \quad & \\
 1490 \quad & \lesssim \sigma^2 \max \left\{ \frac{\sqrt{d \log(1/\delta)}}{n}, \frac{\log(1/\delta)}{n} \right\}, \\
 1491 \quad & \tag{H.3} \\
 1492 \quad &
 \end{aligned}$$

1493 where the last line is valid since $\{\sigma_1^2, \dots, \sigma_d^2\}$ is the eigenvalues of $\hat{\Sigma} = \frac{1}{n} \mathbf{X}^\top \mathbf{X}$ and $\frac{1}{2} \mathbf{I} \preceq \hat{\Sigma} \preceq 2\mathbf{I}$. By Eq.(H.3), we
 1494 obtain that

$$\begin{aligned}
 1495 \quad & \left\| \frac{1}{n} \mathbf{X}^\top \epsilon \right\|_2^2 \geq \mathbb{E} \left[\left\| \frac{1}{n} \mathbf{X}^\top \epsilon \right\|_2^2 \right] - \sigma^2 \max \left\{ \frac{\sqrt{d \log(1/\delta)}}{n}, \frac{\log(1/\delta)}{n} \right\} \\
 1496 \quad & \\
 1497 \quad & = \sigma^2 \sum_{i=1}^d \sigma_i^2 - \sigma^2 \max \left\{ \frac{\sqrt{d \log(1/\delta)}}{n}, \frac{\log(1/\delta)}{n} \right\} \\
 1498 \quad & \\
 1499 \quad & = \sigma^2 \frac{d}{n} - \sigma^2 \max \left\{ \frac{\sqrt{d \log(1/\delta)}}{n}, \frac{\log(1/\delta)}{n} \right\} \tag{by $\frac{1}{2} \mathbf{I} \preceq \hat{\Sigma} \preceq 2\mathbf{I}$ } \\
 1500 \quad & \\
 1501 \quad & \lesssim \sigma^2 \frac{d}{n}, \\
 1502 \quad & \\
 1503 \quad &
 \end{aligned}$$

1504 where the last line is due to $d \geq \mathcal{O}(\log(1/\delta))$. □

1505 Next, we define the event \mathcal{E} as follows:

$$1506 \quad \mathcal{E}_{\text{ridge}} := \left\{ \frac{1}{2} \mathbf{I} \preceq \hat{\Sigma} \preceq 2\mathbf{I}, \left\| \frac{1}{n} \mathbf{X}^\top \epsilon \right\|_2^2 \gtrsim \frac{\sigma^2 d}{n} \right\}.$$

1507 By Lemma H.1, we have $\mathbb{P}(\mathcal{E}) \geq 1 - \delta$ when $n \geq \mathcal{O}(d) \geq \mathcal{O}(\log(1/\delta))$. On $\mathcal{E}_{\text{ridge}}$, we have

$$1508 \quad \mathbb{E}_{\mathbf{w}^*} [\mathcal{E}(\hat{\mathbf{w}}_\lambda)] \gtrsim \frac{\sigma^2 d}{(1 + \lambda)^2 n}. \tag{H.4}$$

1509 When $d \gtrsim n + \log(1/\delta)$, by Lemma F.3, with probability at least $1 - \delta$, we have that $\frac{d}{2} \cdot \mathbf{I} \preceq \mathbf{X}\mathbf{X}^\top \preceq 2d \cdot \mathbf{I}$. Hereafter, we
 1510 condition on this event. By direct calculation, we can decompose the excess risk by

$$1511 \quad \mathbb{E}_{\mathbf{w}^*} [\mathcal{E}(\hat{\mathbf{w}}_\lambda)] = \mathbb{E}_{\mathbf{w}^*} \left\| \left(\mathbf{I} - (\hat{\Sigma} + \lambda \mathbf{I})^{-1} \hat{\Sigma} \right) \mathbf{w}^* \right\|_2^2 + \left\| \frac{1}{n} \cdot (\hat{\Sigma} + \lambda \cdot \mathbf{I})^{-1} \mathbf{X}^\top \epsilon \right\|_2^2.$$

1512 For the first term, we have

$$\begin{aligned}
 1513 \quad & \mathbb{E}_{\mathbf{w}^*} \left\| \left(\mathbf{I} - (\hat{\Sigma} + \lambda \mathbf{I})^{-1} \hat{\Sigma} \right) \mathbf{w}^* \right\|_2^2 = \mathbb{E}_{\mathbf{w}^*} \left\| \left(\mathbf{I} - \mathbf{X}^\top (\mathbf{X}\mathbf{X}^\top + n\lambda \mathbf{I})^{-1} \mathbf{X} \right) \mathbf{w}^* \right\|_2^2 \\
 1514 \quad & \\
 1515 \quad & = \left(1 - \frac{n}{d}\right) \mathbb{E}_{\mathbf{w}^*} \left[\|\mathbf{w}^*\|_2^2 \right], \\
 1516 \quad & \tag{H.5} \\
 1517 \quad & \\
 1518 \quad & = 1 - \frac{n}{d} \\
 1519 \quad & \tag{H.6} \\
 1520 \quad &
 \end{aligned}$$

1521 where the last line is due to $\left(\mathbf{I} - \mathbf{X}^\top (\mathbf{X}\mathbf{X}^\top + n\lambda \mathbf{I})^{-1} \mathbf{X} \right)$ is a $d - n$ space.

$$\begin{aligned}
 1522 \quad & \left\| \frac{1}{n} \cdot (\hat{\Sigma} + \lambda \cdot \mathbf{I})^{-1} \mathbf{X}^\top \epsilon \right\|_2^2 = \epsilon^\top \mathbf{X}\mathbf{X}^\top (\mathbf{X}\mathbf{X}^\top + n\lambda \mathbf{I})^{-2} \epsilon \\
 1523 \quad & \\
 1524 \quad & \geq \frac{dn}{2(2d + n\lambda)^2} \cdot \frac{1}{n} \sum_{i=1}^n \epsilon_i^2, \\
 1525 \quad & \tag{H.7} \\
 1526 \quad & \\
 1527 \quad & \\
 1528 \quad & \\
 1529 \quad & \\
 1530 \quad &
 \end{aligned}$$

1540 where the first line is by $(\mathbf{X}^\top \mathbf{X} + n\lambda \mathbf{I})^{-1} \mathbf{X}^\top = \mathbf{X}^\top (\mathbf{X}\mathbf{X}^\top + n\lambda \mathbf{I})^{-1}$ and the last line is by $\frac{d}{2(d+n\lambda)^2} \cdot \mathbf{I} \preceq$
 1541 $\mathbf{X}\mathbf{X}^\top (\mathbf{X}\mathbf{X}^\top + n\lambda \mathbf{I})^{-2}$. By Tsigler & Bartlett (2023, Lemma 22), we obtain that

$$1542 \left| \sum_{i=1}^n \epsilon_i^2 - n\sigma^2 \right| \lesssim \sigma^2 \sqrt{n \log(1/\delta)} + \sigma^2$$

1546 holds with probability at least $1 - \delta$. When $n \gtrsim \log(1/\delta)$, we have $|\sum_{i=1}^n \epsilon_i^2 - n\sigma^2| \geq \frac{n\sigma^2}{2}$ holds with probability at least
 1547 $1 - \delta$. Taking the union bound, we obtain that

$$1548 \mathbb{E}_{\mathbf{w}^*}[\mathcal{E}(\widehat{\mathbf{w}}_\lambda)] \gtrsim 1 - \frac{n}{d} + \sigma^2 \cdot \frac{dn}{2(2d+n\lambda)^2} \gtrsim 1 - \frac{n}{d} + \sigma^2 \frac{n}{(1+\lambda)^2 d}. \quad (\text{H.8})$$

1552 H.3. Lower Bound for Finite-Step GD

1554 We first consider the case where $n \gtrsim d + \log(1/\delta)$. Define the event \mathcal{E}_{GD} by $\mathcal{E}_{\text{GD}} = \left\{ \frac{1}{2} \cdot \mathbf{I} \preceq \widehat{\Sigma} \preceq 2\mathbf{I} \right\}$. By Lemma F.3,
 1555 $\mathbb{P}(\mathcal{E}_{\text{GD}}) \geq 1 - \delta$. By Eq.(G.4), we have

$$1556 \begin{aligned} \mathbb{E}_{\mathbf{w}^*}[\mathcal{E}(\mathbf{w}_t)] &= \mathbb{E}_{\mathbf{w}^*} \left\| \left(\mathbf{I} - \eta \widehat{\Sigma} \right)^t \mathbf{w}^* \right\|_2^2 + \eta^2 \left\| \left(\frac{1}{n} \sum_{i=1}^t \left(\mathbf{I} - \eta \widehat{\Sigma} \right)^{i-1} \mathbf{X}^\top \epsilon \right) \right\|_2^2 \\ &\geq \eta \left\| \left(\frac{1}{n} \sum_{i=1}^t \left(\mathbf{I} - \eta \widehat{\Sigma} \right)^{i-1} \mathbf{X}^\top \epsilon \right) \right\|_2^2 \\ &= \frac{\eta^2}{n^2} \cdot \left\| \left(\widehat{\Sigma} \left(\mathbf{I} - \left(\mathbf{I} - \eta \widehat{\Sigma} \right)^t \right)^{-1} \right)^{-1} \mathbf{X}^\top \epsilon \right\|_2^2 \\ &\gtrsim \frac{\eta^2}{n^2} \cdot \left\| \left(\widehat{\Sigma} + \frac{1}{\eta t} \cdot \mathbf{I} \right)^{-1} \mathbf{X}^\top \epsilon \right\|_2^2 \\ &\gtrsim \sigma^2 \frac{\eta^2 d}{(1 + 1/(\eta t))^2 n}, \end{aligned}$$

1570 where the second last line is by $\widehat{\Sigma} \left(\mathbf{I} - \left(\mathbf{I} - \eta \widehat{\Sigma} \right)^t \right)^{-1} \preceq \Sigma + \frac{2}{\eta t} \cdot \mathbf{I}$ and the last line is by Eq.(H.4).

1573 We then consider the case where $d \gtrsim n + \log(1/\delta)$. Define the event $\mathcal{E}'_{\text{GD}} = \left\{ \frac{d}{2} \cdot \mathbf{I} \preceq \mathbf{X}\mathbf{X}^\top \preceq 2d\mathbf{I} \right\}$. By Lemma F.3,
 1574 $\mathbb{P}(\mathcal{E}'_{\text{GD}}) \geq 1 - \delta$. Following the proof of Zou et al. (2022, Theorem 4.3), we have

$$1575 \begin{aligned} \mathbb{E}_{\mathbf{w}^*}[\mathcal{E}(\mathbf{w}_t)] &\geq \mathbb{E}_{\mathbf{w}^*} \left\| \left(\mathbf{I} - \mathbf{X}^\top \left(\mathbf{X}\mathbf{X}^\top + \frac{n}{\eta t} \mathbf{I} \right)^{-1} \mathbf{X} \right) \right\|_2^2 + \left\| \frac{1}{n} \mathbf{X}^\top \left(\mathbf{X}\mathbf{X}^\top + \frac{n}{\eta t} \mathbf{I} \right)^{-1} \epsilon \right\|_2^2 \\ &= 1 - \frac{n}{d} + \frac{\sigma^2 n}{\left(1 + \frac{1}{\eta t} \right)^2 d}, \end{aligned}$$

1584 where we use the results from Appendix H.2.

1587 H.4. Lower bound of OLS

1588 Let \mathbf{w}_{ols} be the OLS estimator. It is easy to see $\mathbf{w}_{\text{ols}} = \mathbf{w}_0$. Hence, we have

$$1590 \mathbb{E}_{\mathbf{w}^*}[\mathcal{E}(\mathbf{w}_{\text{ols}})] \gtrsim \begin{cases} \frac{\sigma^2 d}{n} & n \gtrsim d + \log(1/\delta) \\ 1 - \frac{n}{d} + \frac{\sigma^2 n}{d} & d \gtrsim n + \log(1/\delta), \end{cases}$$

1593 holds with probability at least $1 - \delta$.

I. Additional Experiments

Here, we provide additional experiments on the decoder-only architecture and train models with $s = d = 16$.

Training Decoder-Only Transformer In this experiment, we adapt the same input setting and training objective as in (Garg et al., 2023). During training, we set $n = 24$ and $k = 8$ in Eq.(I.1) (where in y_i , we use zero padding to align with \mathbf{x}_i), $d_{\text{hid}} = 256$. We choose $h = 8$ and $l \in \{4, 5, 6\}$.² We then conduct heads assessment experiments on the trained decoder-only transformers with 10 in-context examples, as in the previous settings. The result is shown in Figure 9. We can observe that the decoder-only transformer exhibits the similar weight distribution for each layer as the encoder-based models, indicating that our algorithm may extend to decoder-only based models.

$$\mathbf{E} = \left(\mathbf{x}_1 \ y_1 \ \mathbf{x}_2 \ y_2 \ \dots \ \mathbf{x}_n \ y_n \right), \quad L = \sum_{i=k}^n (\hat{y}_i - y_i)^2. \tag{I.1}$$

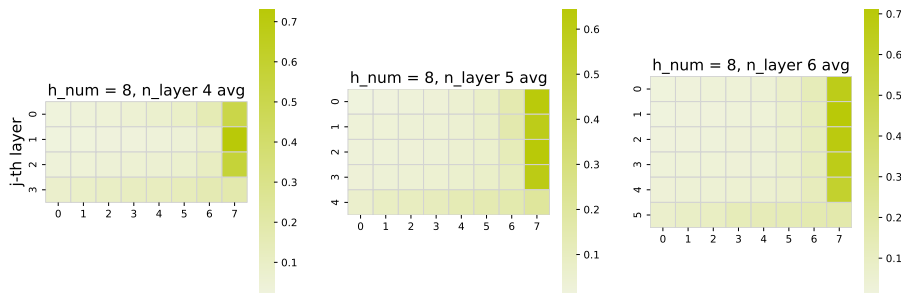


Figure 9: Heads Assessment for decoder-only transformers

Training Models with $s = d = 16$ Here, we adapt the encoder-only transformer and the same settings as introduced in A, but set $s = d = 16$. We observe that in these cases, there is no distinct performance difference between models with different numbers of heads. As shown in Figure 3, when we set $s = 4, d = 16$, transformers with more heads ($h = 4, 8$) always perform better than models with fewer heads ($h = 1, 2$). However, in Figure 10, such a difference is unclear, which aligns well with the theoretical analysis. When s is close to d , a clear better upper bound guarantee, as ensured in cases where $s \ll d$ may not hold.

²We also tried other settings with fewer heads or layers, but even with delicate hyperparameter tuning, decoder-only transformers with fewer heads or layers consistently failed to learn how to solve our sparse linear regression problem. A possible reason is that decoder-only transformers first need to learn the causal structure (Nichani et al., 2024) and then apply an optimization algorithm to the in-context entries, which is more challenging than our encoder-based settings.

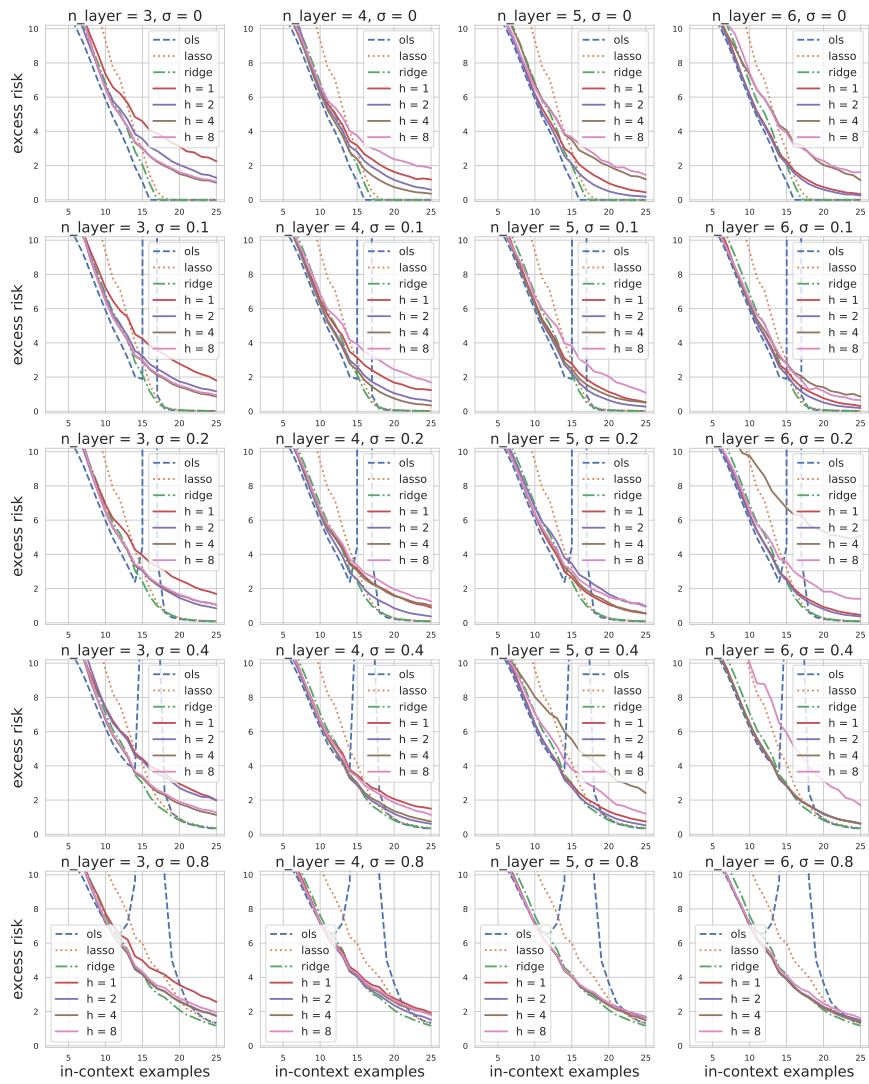


Figure 10: Train Models with $s = d = 16$